The Anatomy of the Normal Heart

1.1 Introduction

Self-evidently, before tackling an abnormal heart, knowledge of normal cardiac anatomy and histology is useful. This chapter examines the structure of the normal heart at the gross, microscopic and ultrastructural levels. Chapter 2 gives details of dissection of the heart and includes a detailed description of sequential segmental analysis. Chapter 3 describes the formation of the normal heart.

A Brief Note on Terminology

As is now common practice in the United Kingdom, I have anglicised many anatomical terms. Thus, for example, I have used the terms "superior caval vein" rather than "superior vena cava" and "arterial duct" rather than "ductus arteriosus". I have, however, baulked at the use of such neologisms as "atriums" and "septums", preferring the original, shorter and infinitely more elegant Latin plurals "atria" and "septa". I fully accept that there is, thus, inconsistency, but it is, at least, consistent inconsistency. The point of language is to communicate information and I do not believe that the terms I have employed in any way impair that communication.

1.2 Anatomy

1.2.1 Situation

The heart sits in the mediastinum, more on the left side than the right. Inferiorly it rests on the central part of the diaphragm and superiorly the aortic arch rises almost to the neck (Figures 1.1 and 1.2). Posteriorly, there is the descending thoracic aorta, oesophagus and vertebral column, and anteriorly, the thymus and sternum. The lungs lie on either side, and their anterior extensions interpose between the heart and the anterior chest wall.

1.2.2 Pericardium

The heart is anchored by its attached structures (caval and pulmonary veins and the aorta and pulmonary trunk) and is surrounded by a dense fibrous covering – the pericardium. The pericardium encloses the heart and great vessels but is reflected off the anchoring structures (Figure 1.3). Externally, the parietal layer of pericardium is adherent to the diaphragm, sternum and costal cartilages. The bilateral symmetry of the pulmonary veins combined with asymmetrical arrangement of the caval veins (lying on the right side, and not the left) means that there is a blind invagination of pericardium behind the left atrium between the right pulmonary veins and the inferior caval vein – the oblique sinus of the pericardium (Figure 1.4). A transverse sinus runs from side to side posterior to the aorta and pulmonary trunk and anterior to the bodies of both atria (Figure 1.5).
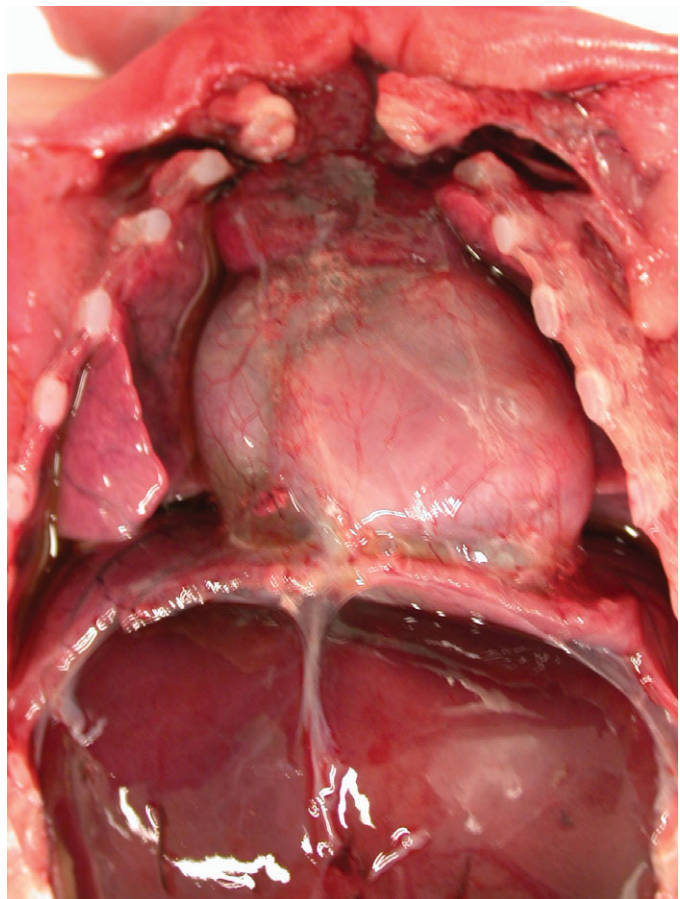

Figure 1.1 Normal heart. A post-mortem in a neonate. The chest has been opened and the sternum removed by cutting through the costal cartilages. The heart is enclosed in the pericardium. Above is the thymus, below the diaphragm separates it from the liver. The pleural cavities are open, and the lungs are visible.
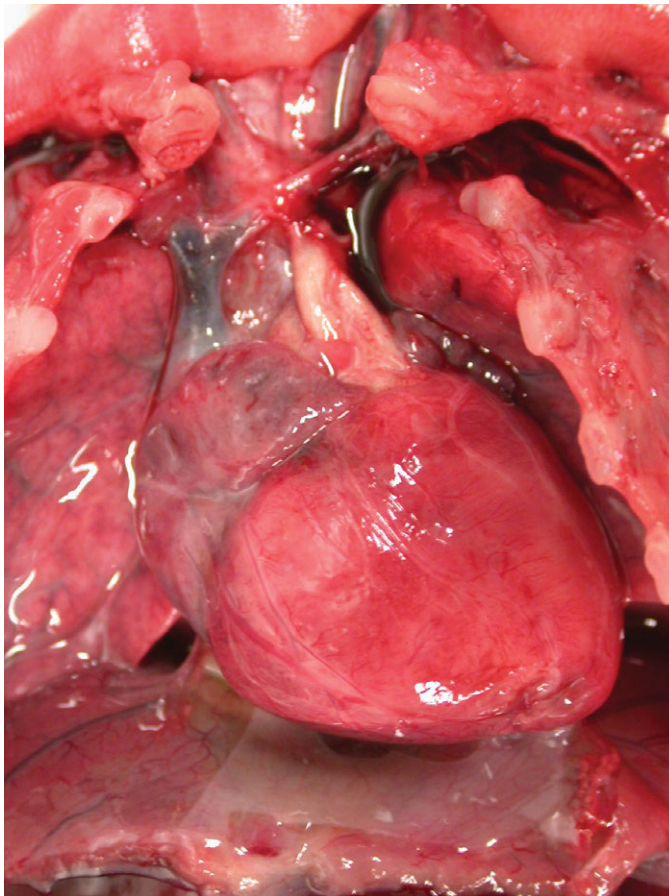
Figure 1.2 Normal heart after removal of the thymus and pericardium. The greater part of the ventricular mass visible in this view is the right ventricle. The right atrial appendage lies above, and above this again the superior caval vein. The pulmonary artery arises from the right ventricle, and the aorta is just visible behind it. The left atrial appendage is just visible to the left of the arterial pedicle.
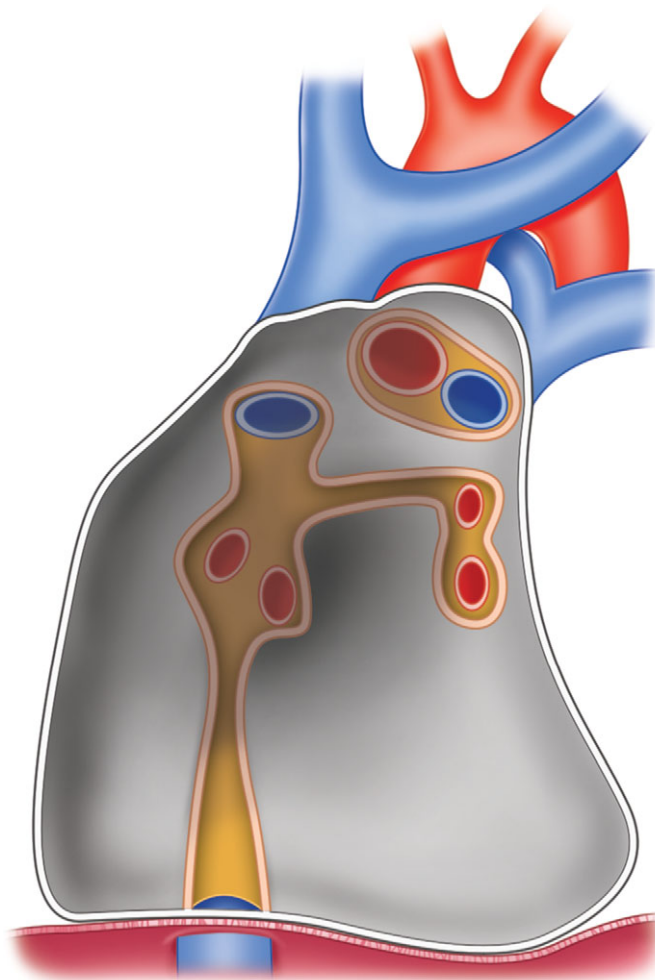

Figure 1.3 Diagram of attachments of pericardium. The sites of attachment are coloured red. The pericardial cavity encloses the most proximal parts of the superior and inferior caval veins and the pulmonary veins, and also the most proximal parts of the aorta and pulmonary trunk and proximal part of the arterial duct.
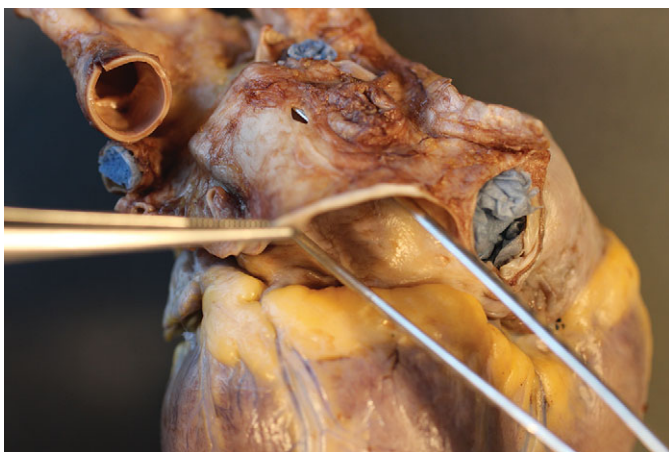

Figure 1.4 Oblique sinus of the pericardium. The heart viewed from behind. One pair of forceps grabs the cut edge of the parietal pericardium. Another pair is inserted into the oblique sinus. The right margin is formed by the pericardial attachment between the inferior caval vein and right pulmonary veins, and the superior blind end is closed by the attachment of pericardium between the upper pulmonary veins.

Figure 1.5 Transverse sinus of pericardium. The heart is viewed from the right side. A pair of forceps has been inserted from the left side between the arterial pedicle and the atria. The tip can be seen emerging on the right side between the junction of the superior caval vein and right atrium posteriorly and the aorta anteriorly. The cut edge of the pericardial reflection is seen above.

A small triangular fold of the pericardium is reflected from the left pulmonary artery to the left upper pulmonary vein – the fold of the left caval vein (vestigial fold of Marshall) (Figure 1.6). It contains a fibrous strand, called the ligament of the left caval vein, that is a remnant of the left common cardinal vein (left duct of Cuvier) and that extends downwards in front of the root of the left lung to the back of the left atrium where it is continuous with the oblique vein of the left atrium. The fold frequently forms the anterior wall of a small blind recess, the mouth of which is directed to the left. In the undissected state connective tissue joins the aorta and pulmonary trunk, and there is no cavity between them. The pulmonary end of the arterial duct lies within the pericardial cavity; its distal part is outwith the pericardium. The pericardium is not essential to life, nor the efficient working of the heart, which operates adequately even when the pericardium is removed. The phrenic nerves descend on the outer lateral aspects of the pericardial sac, one on each side.

1.2.3 The Right and Left Atrium

The right atrium comprises three components: a smooth-walled venous component; an atrial appendage; a vestibule supporting the tricuspid valve.

1. The venous component lies between the orifices of the superior and inferior caval veins, encompasses the orifice of the coronary sinus and is smooth walled (Figure 1.7). Embryologically it derives from the sinus venosus and is separated from the atrial appendage externally by the terminal groove and internally by the terminal crest (crista terminalis) (Figure 1.8). The terminal crest originates on the right atrial aspect of the interatrial septum and passes anterior to the mouth of the superior caval vein onto the lateral wall of the atrium and extends downwards to pass anterior to the orifice of the inferior caval vein where it is continuous with the eustachian valve.

2. The right atrial appendage is triangular in shape and has a broad junction with the atrium (Figure 1.9). It contains multiple parallel trabeculations – pectinate muscles – that extend around the greater part of the orifice of the tricuspid valve and are limited by the terminal crest (Figure 1.8). Externally, the junction of the crest of the appendage with the superior caval vein marks the site of the sinoatrial node (Figure 1.10).

3. The vestibule supports the tricuspid valve, and it is smooth. Situated in the vestibule, between the orifice of the coronary sinus, the attachment of the tricuspid valve and the membranous septum (see Section 1.2.7), lies the
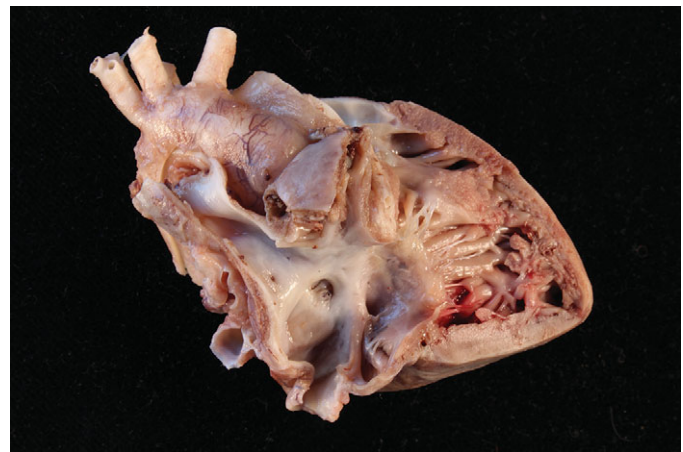

Figure 1.6 Fold of Marshall. The heart viewed from the left side and displaced by forceps to the right to display the left pulmonary artery and the left pulmonary veins. A fold of pericardium runs from the inferior surface of the left pulmonary artery to the upper border of the left upper pulmonary vein. This is the vestigial fold of Marshall, and it is continuous with the oblique vein of the left atrium (not visible in this picture). The transverse sinus of the pericardium lies anterior to the fold. Posterior to it is a blind-ending recess of the pericardial cavity.

Figure 1.7 The right heart dissected to show the septal structures. The parts of the right atrium shown lie between the orifices of the superior and inferior caval veins. Visible are the interatrial septum, including oval fossa, vestibule of the tricuspid valve, and coronary sinus orifice. In this view only the origin (just above the oval fossa) and insertion (from the junction with the inferior caval vein, eustachian valve, and above the coronary sinus) of the terminal crest are seen, and the muscular trabeculations and appendage are not included. This part of the atrium derives from the sinus venosus and is smooth walled.

atrioventricular (AV) node. The bundle of His exits the node anteriorly to penetrate the membranous septum and divide astride the crest of the muscular interventricular septum giving rise to the right and left bundle branches.

The interatrial septum is smaller than it appears. The true septum comprises only the oval fossa with its rim (Figure 1.11). The remainder of the party wall with the left atrium is formed by infolding of both atrial walls with a sandwich of extracardiac adipose tissue (Figure 1.12). The oval fossa is closed by a flap valve. About 20% of the population have a valve that is
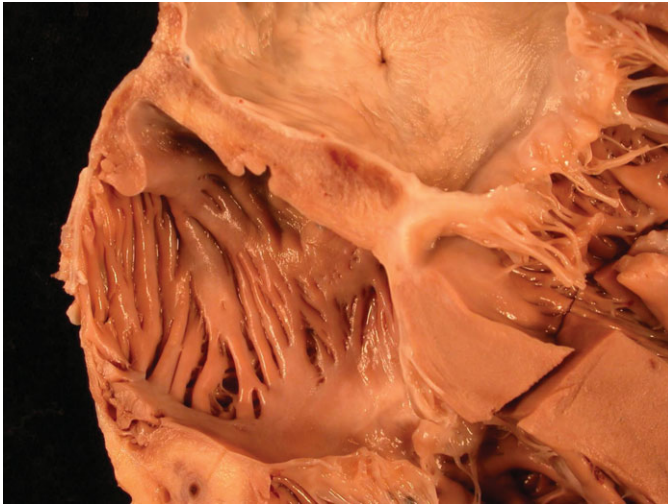

Figure 1.8 Terminal crest. The right atrium in a simulated four-chamber view of the heart. The interatrial septum runs diagonally across the field. A little beneath it, and separated from it by the orifice of the superior caval vein (not seen in this view), is the terminal crest – a solid rounded bar of atrial muscle that runs from superior to inferior delimiting the atrial appendage, and from which muscular trabeculations arise at right angles and extend to the vestibule of the tricuspid valve.
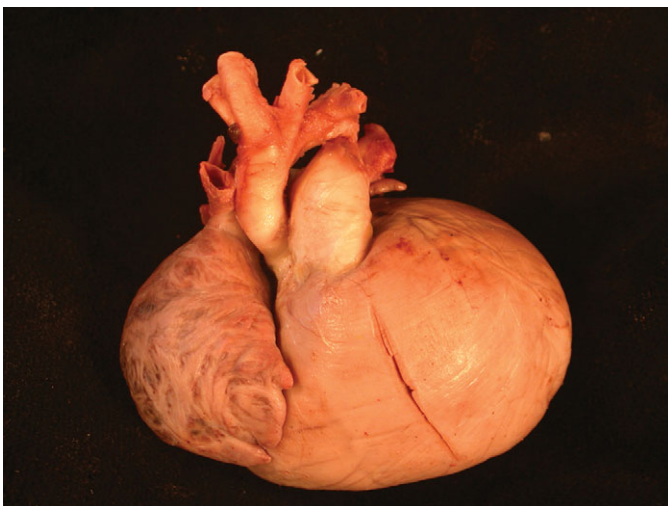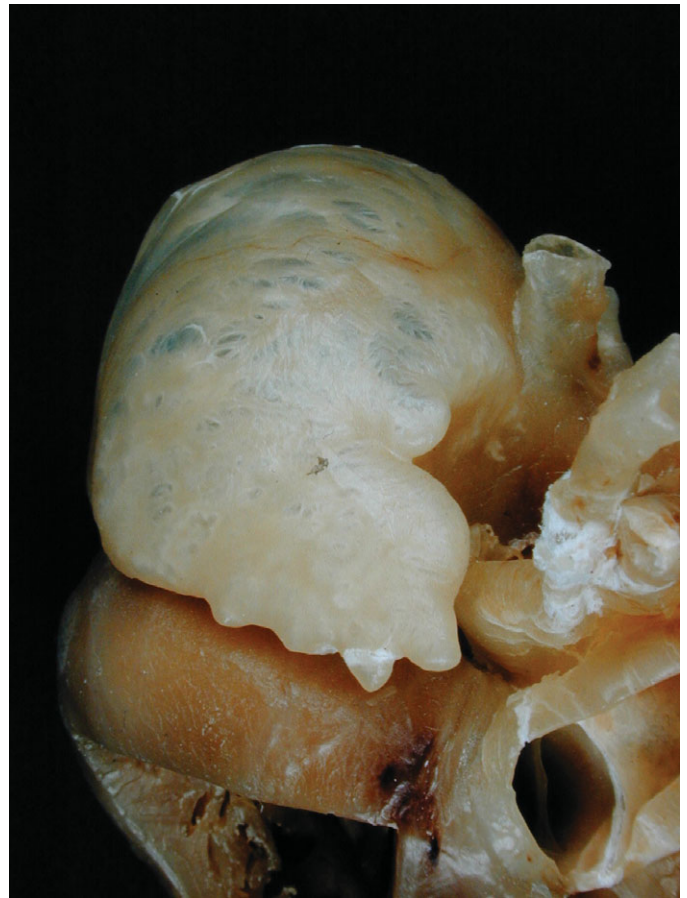

Figure 1.9 Right atrial appendage. Viewed from the outside. The right atrial appendage is roughly pyramidal in shape, has a broad junction with the right atrium and contains parallel muscular trabeculations that extends into the body of the atrium around the vestibule of the tricuspid valve.
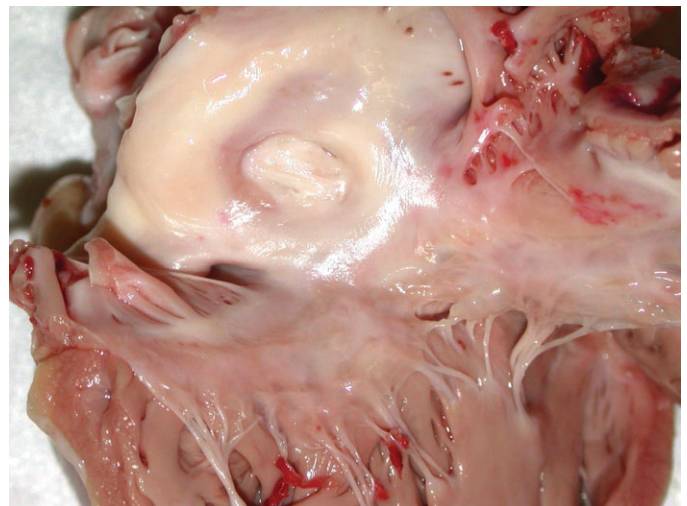

Figure 1.10 The sinoatrial node lies at the junction of the superior caval vein and the crest of the right atrial appendage.

Figure 1.11 Oval fossa. The right atrium and right ventricle have been opened, and the heart is viewed from the right side. The opened orifice of the inferior caval vein is to the left midfield and the unopened orifice of the superior caval vein to the upper midfield. Lying between them is the oval depression of the oval fossa. Its rim is smooth and the flap valve completely closed. Beneath it, the orifice of the coronary sinus can be seen.

(A)
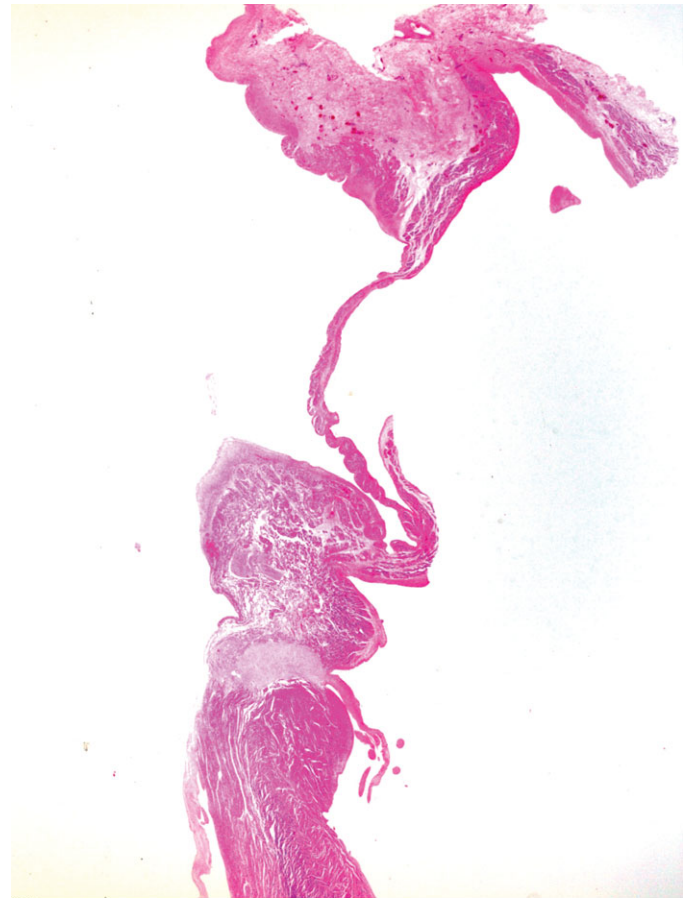
(B)

Figure 1.12 Infolding of atrial septum. **(A)** A post-mortem heart from a case of idiopathic dilated cardiomyopathy showing the interatrial septum cut vertically through the oval fossa. The rim of the fossa is muscular, but the remainder of the apparent septum is formed of infolding of extracardiac fibrous and adipose tissue. Note also the extension of muscular trabeculations around the right atrioventricular junction while the left is smooth. **(B)** The histological section shows more clearly the infolding of fibrous tissue between the two atrial walls, especially superiorly. The right atrium is on the left of the field and the left atrium to the right.
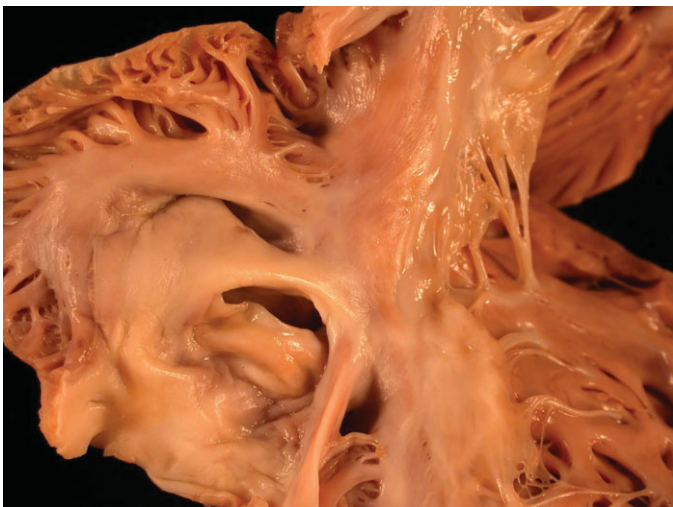

Figure 1.13 The right atrium and ventricle have been opened and are viewed from the right side. The opened right atrial appendage is on top. Beneath this is the slightly distorted orifice of the superior caval vein. Beneath this again is the oval fossa. There is persistence of the oval foramen with the flap valve not closing the defect anterosuperiorly.

probe patent at its anterosuperior margin (sometimes termed persistent foramen ovale (PFO)) (Fig 1.13).

The right atrium contains a eustachian valve of variable prominence (Figure 1.7) – a relic of the structure that in fetal life directed the venous duct (ductus venosus) blood from the inferior caval vein through the oval foramen. In some instances, the valve is a thick muscular ridge. The coronary sinus may be guarded by a thin membrane: the thebesian valve. The valve is usually attached at the postero-inferior margin and is variably fenestrated (Figure 1.14). The area between the orifices of the inferior caval vein and the coronary sinus is termed the sinus septum and is traversed by the tendon of Todaro. Between the eustachian valve and the attachment of the septal leaflet of the tricuspid valve is an area known by electrophysiologists as the isthmus. It contains a pouch-like area beneath the orifice of the coronary sinus termed the sub-thebesian recess [1].

A Chiari network may be present (Figure 1.15). This is a netlike structure in the right atrium connected to the terminal crest or atrial septum and to the eustachian or thebesian valve.

Figure 1.14 Eustachian and thebesian valves. **(A)** The right atrium and ventricle have been opened and are viewed from the right side. The oval fossa is at the top of the picture. The eustachian valve runs obliquely from bottom left to upper centre. Towards its upper extent is the oval fossa with a slight ridge of tissue postero-interiorly forming the thebesian valve. The valve is very variable in morphology, if it is present at all. **(B)** In a different heart viewed from the same vantage point, the eustachian valve has been grasped and pulled taut. It can be appreciated how it acts as a baffle to direct blood to the oval fossa. The coronary sinus shows a fenestrated thebesian valve.
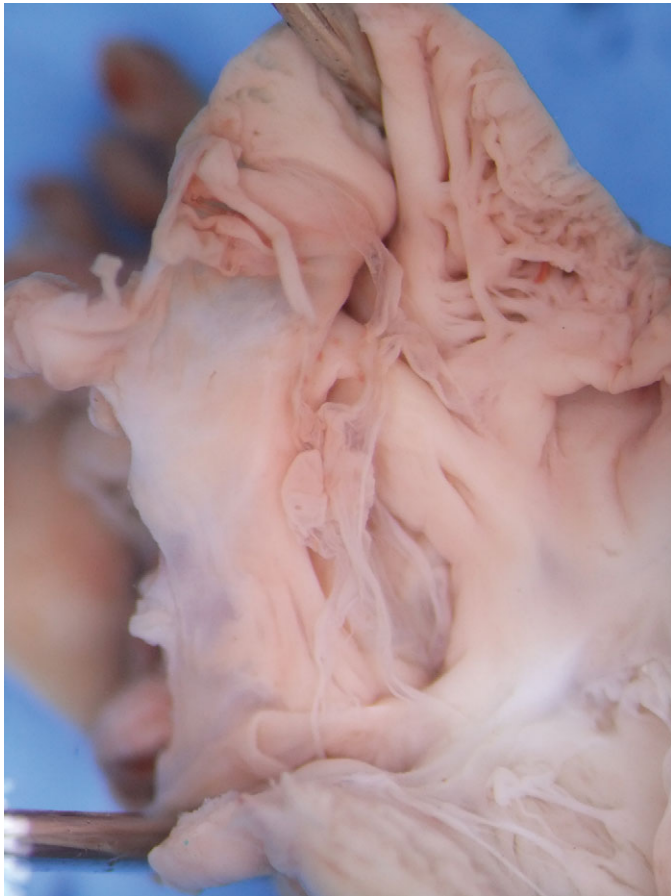

Figure 1.15 Chiari network. Termination of pregnancy at 18 weeks' gestation for hypoplastic right heart. The right atrium has been opened looking towards the interatrial septum. A filigreed diaphanous structure partly covers the oval fossa extending from the terminal crest down towards the eustachian and thebesian valves. The right heart structures were small but otherwise unremarkable. It is unknown whether this Chiari network was the cause of right heart hypoplasia by obstructing the tricuspid orifice.

Usually it is highly fenestrated, but may be more solid and resemble a spinnaker sail, causing obstruction to forwards flow of venous blood across the tricuspid valve [2]. It represents the remains of the right venous valve of the sinus venosus [3].

Remnants of the left valve of the sinus venosus may be seen as lacelike structures or cords resembling tendinous cords (chordae tendineae) attached to the right side of the atrial septum in the region of the oval fossa (Figure 1.16) [4].

The left atrium is usually smaller than the right and receives the pulmonary veins. The junction between the two is marked externally by a shallow groove running vertically between the superior caval vein and the right pulmonary veins – Waterston's groove (Figure 1.17). Usually there are four: two on the right – one superior and one inferior – and two on the left – one superior and one inferior – but the number can vary. The left side of the oval fossa is generally corrugated and rougher than on the right (Figure 1.18). The endocardium of the left atrium is thicker than that of the right atrium, the thickening being caused by fibroelastic tissue. This should not be mistaken for a pathological change. The left atrial appendage is quite distinct from the right. It is long and tubular and has a narrow junction with the atrium and characteristically has a hooked extremity. Pectinate muscles are confined to the appendage and do not extend onto the atrial wall, nor around the orifice of the mitral valve (Figure 1.19). The coronary sinus runs in the posterior wall of the left atrium at the level of the atrioventricular junction. If there is a persistent left superior caval vein, the sinus is correspondingly larger and may bulge into the left atrium.

1.2.4 The Ventricles

The left ventricle is the thicker walled of the two ventricles and is ellipsoid in shape. The right ventricle is wrapped around its rightward aspect, thus giving it a more complex

Figure 1.16 Remnants of left valve of sinus venosus. The oval fossa viewed from the right atrium. The eustachian valve is grasped by forceps. The lower border of the oval fossa is buttressed by a trabecular network of fibrous cords that represent the incompletely fused remnants of the left valve of the embryonic sinus venosus.
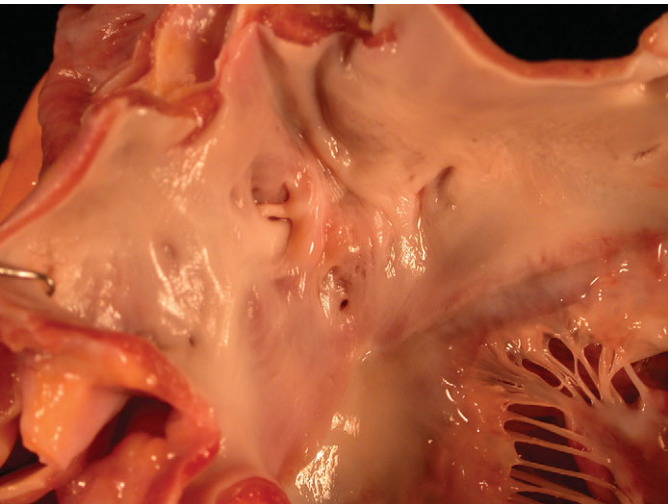

Figure 1.18 Left side oval fossa. The left atrium has been opened to display the left side of the interatrial septum. The mitral valve leaflets are apparent to the lower right. Note the opaque thick pale endocardium characteristic of the left atrium. This is especially evident on the cut edge of the wall at the upper right of the field where the endocardium occupies nearly one-third of the thickness of the atrial wall. No distinct oval structure can be recognised on the left side of the septum. Instead the attachments of the flap valve of the oval fossa are evident as a rugose area in the centre of the field.

Figure 1.17 Waterston's groove. The heart viewed from behind. Running superiorly from the inferior caval vein to the superior caval vein is a shallow groove marking the junction between the right and left atrium – Waterston's groove.

shape (Figure 1.20). From the point of view of descriptive anatomy, the ventricles have three components: an inlet, comprising the atrioventricular valve and its supporting structures; an outlet supporting the arterial valve; and an apical trabecular component linking the two (Figure 1.21). It is important to keep in mind that the components on the right and left side are not perfectly aligned. This apical trabecular component is the most constant and most characteristic feature of the ventricles. On the right side, the septal aspect of the apex shows thick muscle bundles termed trabeculations (trabeculae) that have a roughly parallel orientation along the long axis of the septum. The most prominent of these, the septomarginal trabeculation (trabecula septomarginalis), extends nearly the full length of the septum. Shaped like the letter Y, its stem extends from the apex upwards, its anterior limb extends in the outflow tract to the pulmonary valve and its posterior limb extends backwards, supporting the medial papillary muscle of the tricuspid valve (Figure 1.22). There is considerable normal variation in the posterior limb – in some cases it extends posterior to the membranous septum and in others anterior [5]. The septomarginal trabeculation is usually incorporated into the muscle of the septum analogous to an engaged pillar or pilaster, but may occasionally, at least in the fetus, be a largely free-standing structure (Figure 1.23). On the left side of the septum the trabeculations are fine and typically have an interwoven appearance, and the outflow tract shows a smooth septal surface (Figure 1.24).
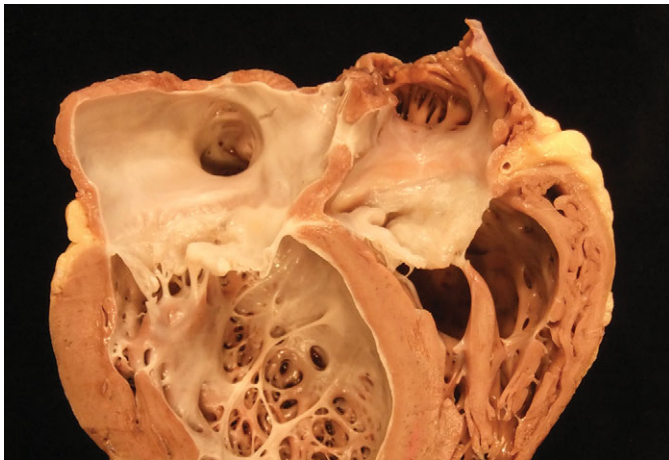
7

Figure 1.19 Left atrial appendage. Explanted heart from a 14-year-old boy with idiopathic dilated cardiomyopathy, cut in a four-chamber view and viewed from behind. The orifice of the right atrial appendage is on the right side and shows extension of the muscular trabeculations from the appendage around the atrioventricular junction. By contrast, on the left side, the junction of the appendage and atrium is narrow and the trabeculations are confined to the appendage, the remainder of the atrial wall being smooth.
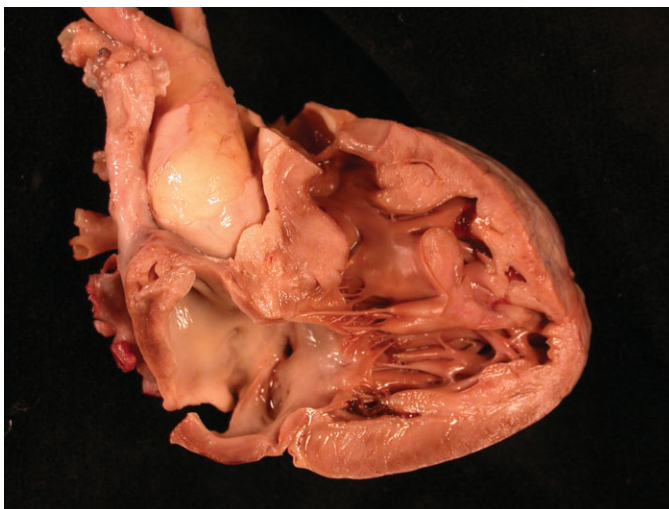

Figure 1.20 Right ventricle wrapping around left. A short-axis dissection of the heart viewed from the apical aspect. The left ventricle is roughly elliptical in cross section and is at the lower aspect of the picture. The anterior leaflet of the mitral valve occupies much of its cavity. The right ventricle is wrapped around the left and extends from the left of the picture, where the right atrium and tricuspid valve are seen to the right, where it disappears up towards the pulmonary valve. Occupying the "hinge" region is the supraventricular crest. The bulge upwards in the interventricular septum at the site of insertion of the supraventricular crest into the septum represents the stem of the septomarginal trabeculation. The anterior limb of the septomarginal trabeculation extends upwards into the right ventricular outflow tract. The posterior limb is obscured by anterior and septal leaflets of the tricuspid valve. The commissure of the valve is supported by the medial papillary muscle attached to the posterior limb.
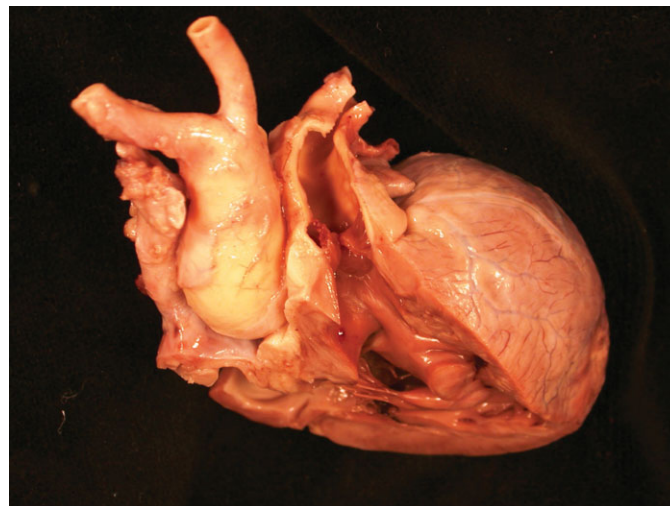

Figure 1.21 Components of septal aspect of right ventricle. The heart has been dissected to demonstrate the right-sided aspect of the interventricular septum. The tricuspid valve together with its tension apparatus (tendinous cords and papillary muscles) occupies the inlet component. Distal to it is the apical trabecular component where the muscular trabeculations are chunky and roughly parallel to one another. The outlet component lies superior to the papillary muscles of the tricuspid valve and is largely smooth. The septomarginal trabeculation occupies much of this component.

Figure 1.22 Septomarginal trabeculation. The same dissection as in Fig 1.21 rotated forwards to demonstrate the right ventricular outflow tract. The Y-shape of the septomarginal trabeculation can be readily appreciated with the anterior limb of the Y extending up to the pulmonary valve. Inserted between the limbs of the Y is the supraventricular crest, which separates the pulmonary valve from the tricuspid valve and which forms the posterior wall of the subpulmonary infundibulum. Externally, the right coronary artery travels along the upper border of the supraventricular crest. Note the spiral configuration of the aorta and pulmonary artery relative to each other.

1.2.5 Atrioventricular Valves

The right-sided atrioventricular valve, the tricuspid valve, as its name indicates, has three leaflets: septal, anterosuperior and inferior. All three leaflets are anchored by tendinous cords (chordae tendineae) to papillary muscle groups situated at the leaflet commissures. The septal leaflet is also attached by cords directly to the septum (Figure 1.25). Its medial papillary muscle (muscle of Lancisi) is small and arises from the

posterior limb of the septomarginal trabeculation (Figure 1.20). Frequently there are associated small accessory papillary muscles variably located around the muscle of Lancisi [5]. The anterosuperior leaflet is the largest of the three leaflets of
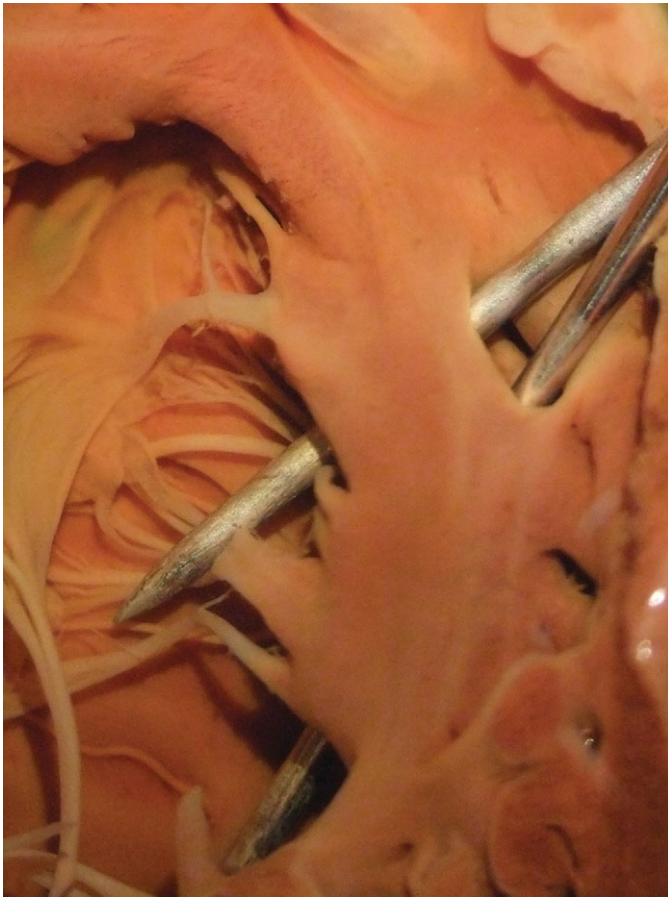
Figure 1.23 Free-standing septomarginal trabeculation. A fetus of 24 weeks' gestation with hypoplastic left heart. The dissection of the right side of the interventricular septum shows a septomarginal trabeculation that is largely free standing. Pins have been inserted between the stem of the trabeculation and the septum to demonstrate the lack of attachment.

Figure 1.24 Septal aspect of left ventricle. The left ventricle has been opened along its lateral margin and splayed to demonstrate the structures on the left aspect of the interventricular septum. The inlet component is occupied by the mitral valve leaflets, their attached tendinous cords and papillary muscles. The apical component shows fine trabeculations with a criss-cross configuration. The outlet component is smooth.

the tricuspid valve and its anterior papillary muscle is prominent. The inferior leaflet is less conspicuous, as are its papillary muscles.

The left atrioventricular valve – the mitral valve – comprises two leaflets: a large rectangular, anterior (or aortic) leaflet, and a mural leaflet, which is attached to about two-thirds of the atrioventricular junction (Figure 1.26). Two large papillary muscle groups, termed anterolateral and posteromedial, support the commissures of the leaflets. The anterior leaflet is attached to the interventricular septum only on its postero-inferior aspect; the left ventricular outflow tract is interposed between the ventricular aspect of the leaflet and the septum. Thus, there is fibrous continuity via a subaortic fibrous curtain between the anterior mitral leaflet and the non-coronary cusp and part of the left coronary cusp of the aortic valves (Figure 1.27). The two lateral margins of this area of fibrous continuity show fibrous thickening, the so-called right and left fibrous trigones, the right fibrous trigone being in continuity with the membranous septum and the left fibrous trigone anchoring the fibrous curtain to the muscular septum.
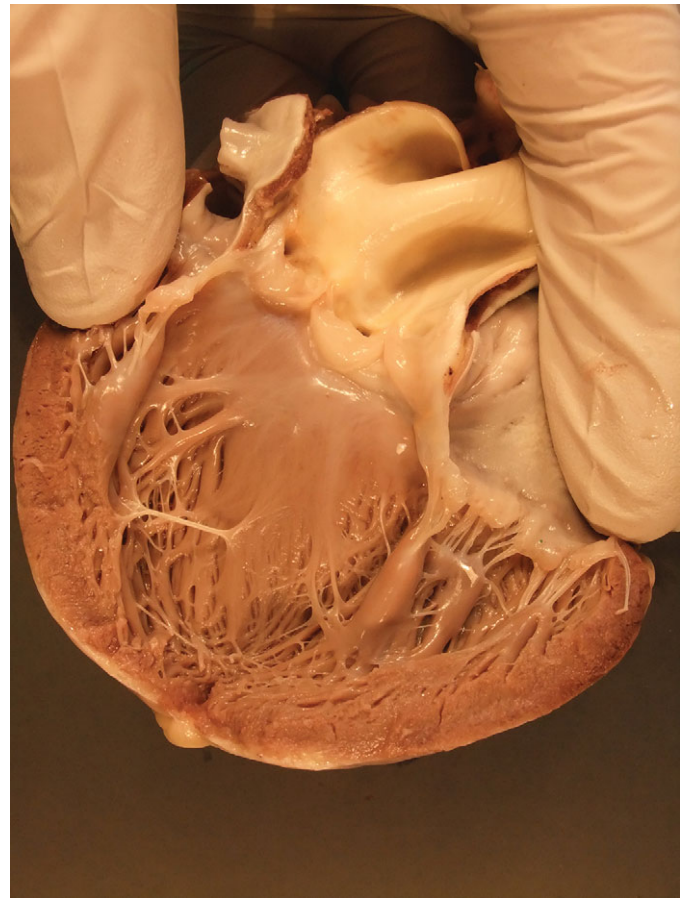
In a small percentage of normal hearts a small band of muscle separates mitral and aortic valves [6].

The attachment of the mitral valve to the left side of the interventricular septum is higher than the attachment of the tricuspid valve to the right side of the septum, a feature termed offsetting, and easily detected on echocardiography and useful for identifying the ventricles (Figure 1.28). This means that there is an area between the two attachment sites where there is a potential communication between the left ventricle and the right atrium – the so-called atrioventricular septum.

Especially in the neonate, small blood-filled cysts may be present on the leaflets of the atrioventricular valves (see Section 1.3.4 for more detailed discussion). Yellow thickenings may be seen on the anterior leaflet of the mitral valve even at a young age (Figure 1.27) [7].

1.2.6 Interventricular Septum

The septum between the two ventricles is predominantly muscular and usually of a similar thickness to the rest of the left
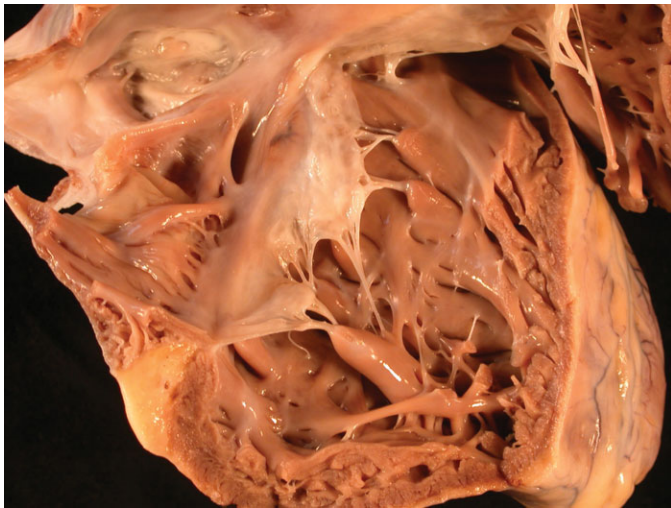
Figure 1.25 Tricuspid valve. A heart opened to display the tricuspid valve. The septal leaflet, as its name implies, is attached to the spetum and shows short cord-like attachments to it. The medial papillary muscle is a small structure at the top centre of the field. The inferior leaflet has been cut through to open the heart. Nonetheless, its papillary muscle is visible towards the bottom centre. The anterosuperior leaflet is the largest and occupies the upper right field. Its papillary muscle is just visible.
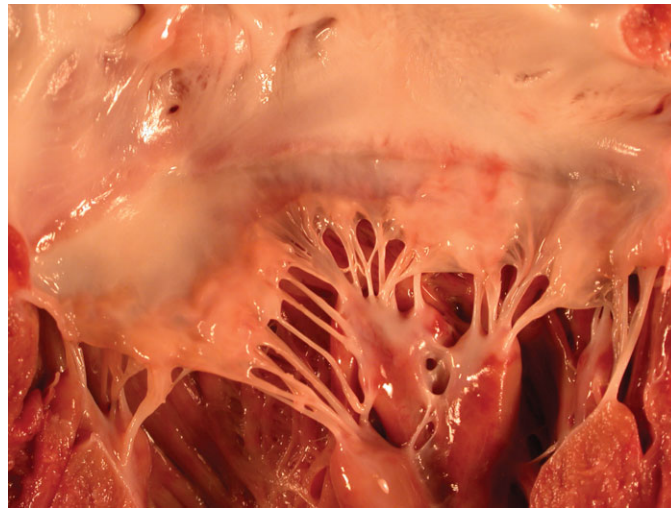

Figure 1.26 Mitral valve. The mitral valve has been opened between the lateral junction of the anterior leaflet (to the left of the field) and the mural leaflet. The posteromedial papillary muscle group occupies the centre of the field and the anterolateral group has been divided with components on the extreme right and left of the lower part of the field. Note that the anterosuperior leaflet is attached to about only one-third of the valve circumference but has a greater depth. Thus, when closed, the anterosuperior leaflet occupies the greater part of the cross sectional area of the orifice and is encompassed on three sides by the mural leaflet.
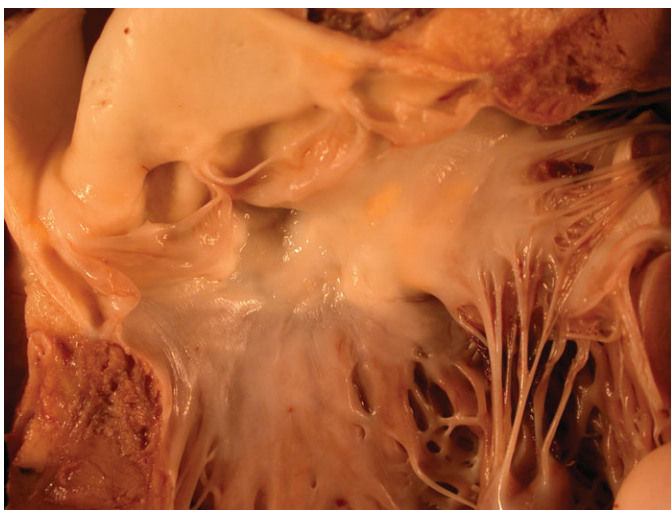

Figure 1.27 Subaortic fibrous curtain. The left ventricular outflow tract has been opened and the anterosuperior leaflet of the mitral valve retracted to the right of the field. The proximal aorta, aortic valve and septal aspect of the left ventricular outflow are visible. The cut passes through the left coronary cusp of the aortic valve. The two intact leaflets are the right coronary leaflet to the left of the field and the non-coronary leaflet in the centre. In the fibrous triangle between the right and non-coronary cusps lies the membranous septum. The mitral valve is in fibrous continuity with the non-coronary cusp and part of the left coronary cusp – the so-called subaortic fibrous curtain. That part of the fibrous curtain adjacent to the membranous septum is thickened as the right fibrous trigone. The left fibrous trigone attaches to the muscular interventricular septum. Note that even though this child was only five years old at the time of death, there are fatty streaks in the fibrous curtain.

Figure 1.28 Tricuspid–mitral offsetting. Heart cut in a simulated four-chamber view. The anterosuperior leaflet of the mitral valve is attached to the septum at a higher level than the septal leaflet of the tricuspid valve. The area of the septum lying between the two attachments is the atrioventricular septum.

ventricular wall. The right ventricular aspect has already been discussed in detail above. The left ventricular aspect has a finely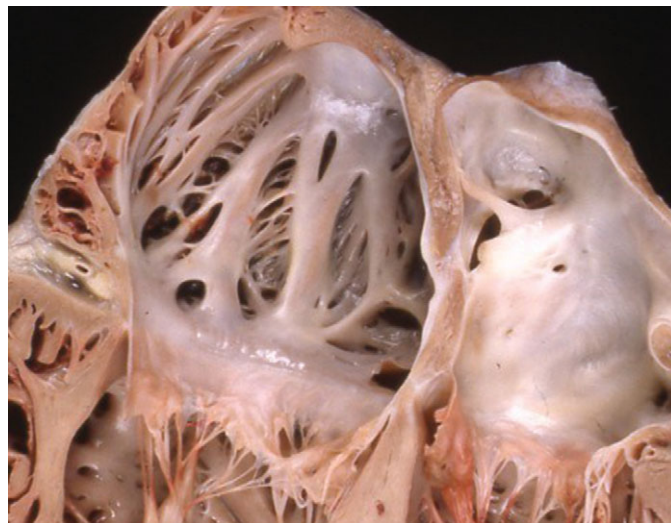 trabeculated apical aspect. The upper part of the left side of the interventricular septum is usually smooth and forms the left ventricular outflow tract (Figure 1.24). In this area and immediately beneath the aortic valve there is a small fibrous area situated between the right and non-coronary cusps of the aortic valve and extending beneath the non-coronary cusp, where the septum is very thin and completely fibrous – the membranous septum (Figure 1.29). This can be dramatically demonstrated by transillumination (Figure 1.30). On the right

Figure 1.29 Membranous septum. A close-up view of the left ventricular outflow tract. The anterosuperior leaflet of the mitral valve has been bisected to expose the septal aspect of the outflow tract. On the left upper part of the picture the right coronary cusp of the aortic valve is visible with the orifice of the right coronary artery. The non-coronary cusp lies beside it towards the mitral valve. In the triangle formed by the ventricular attachments of these two cusps and the crest of the muscular interventricular septum lies the membranous septum. The right fibrous trigone lies beside it, representing the thickened right end of the subaortic fibrous curtain.

Figure 1.30 Membranous septum. The left ventricular outflow tract opened in the same manner as in Figure 1.29 and transilluminated from the right side. This demonstrates the thin membranous septum that is roughly triangular in shape and occupies the triangle between the ventricular attachments of the right and non-coronary cusps of the aortic valve.

Figure 1.31 Relationship of the septal leaflet of the tricuspid valve to the membranous septum. The heart is viewed from the right side – the endocardium of the right atrium is stripped and the leaflets of the tricuspid valve cut close to their attachments to the atrioventricular junction. The right atrium occupies the left and upper parts of the field and the right ventricle the lower and right parts. The atrioventicular junction runs diagonally from upper right to lower left. At the very centre of the field the membranous septum can be seen as a pale grey triangular area. It is crossed by the attachment of the tricuspid valve leaflet such that a small part lies above the valve (to the left in this picture). This is the membranous atrioventricular septum.

Figure 1.32 Membranous septum in trisomy 21. A heart from a child with trisomy 21 viewed from the right side. The membranous septum is in the centre of the field, and the commissure of the septal and anterior leaflets is deficient, exposing a large membranous septum.

side, the attachment of the septal leaflet of the tricuspid valve runs diagonally across this membranous septum (Figure 1.31). The membranous septum may be abnormally large in cases of trisomy 21 (Figure 1.32) [8].

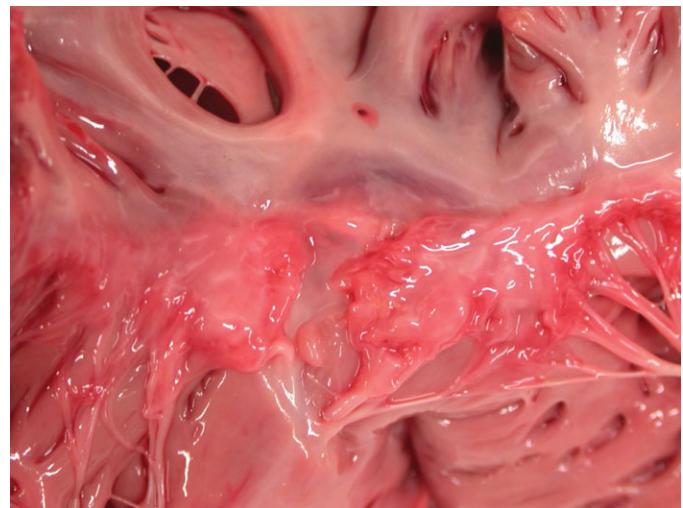The exact anatomy of the muscle bundles in the normal heart has not been conclusively proven. At least in the fetal heart the arrangement has been described as "a set of geodesics arranged over nested toroids" and has been likened to a set of distorted pretzels or sets of two doughnuts side by side, the interventricular septum corresponding to the junction of the two doughnuts [9]. The right ventricle contributes more to the distortion because of the separation of tricuspid and pulmonary valve (Figure 1.33).

1.2.7 Cardiac Conduction System

There are two main recognisable components to the human cardiac conduction system: the sinoatrial node and the atrioventricular conduction axis [10]. It is still debated as to
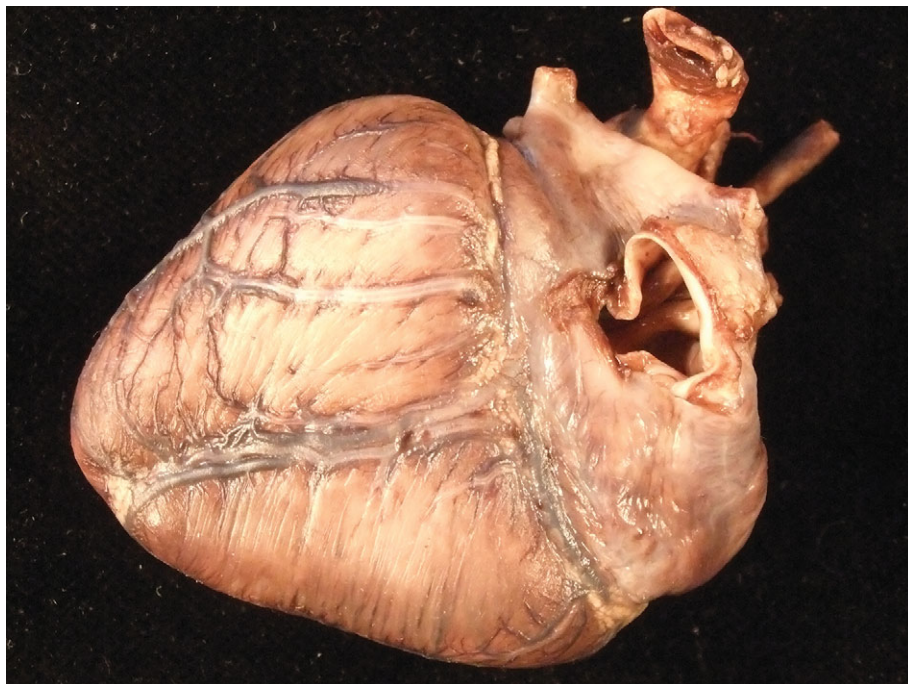
11

Figure 1.33 Orientation of muscle bundles of the ventricles. A female infant born at term who died very shortly afterwards from pulmonary hypoplasia. The heart is viewed from posteriorly. The orientation of the superficial muscle bundles in the ventricular myocardium is evident on the epicardial surface. The orientation is oblique but slightly different in its axis in both ventricles and dips in towards the interventricular septum.

whether anatomically distinct specialised conduction pathways exist in the right atrium linking the two [11, 12].

The sinoatrial node is roughly triangular in outline and lies on the epicardial surface of the heart at the junction of the superior caval vein with the crest of the right atrial appendage, sometimes in front of the junction, sometimes behind and, at times, astride it. It is not visible macroscopically (Figure 1.10) and requires histological examination for its assessment.

The AV node is also roughly triangular in shape and sits at the lower part of the interatrial septum in the triangle of Koch. The borders of this triangle are the atrioventricular junction, the mouth of the coronary sinus and the tendon of Todaro – a fibrous subendocardial prolongation of the eustachian valve that inserts into the membranous septum (Figure 1.34). The non-branching bundle of His emerges from the node, penetrates the membranous septum and divides astride the crest of the muscular interventricular septum to give a fan-shaped left bundle branch and a rather more discrete right bundle branch. The left bundle branch lies, for the most part, immediately beneath the endocardium of the left ventricular outflow tract, by contrast, the right bundle branch dives into the myocardium of the right side of the interventricular septum and travels towards the apex in that location [13]. The structure is dealt with in more detail in Section 1.3.5.

1.2.8 Arterial Valves

The pulmonary artery arises from the right ventricle, and the aorta from the left. The aortic valve sits in the centre of the base of the heart and is wedged between the tricuspid and mitral valves (the axes of both atrioventricular valves being at an angle of approximately 45 degrees to the anteroposterior

Figure 1.34 Triangle of Koch. Same heart as in Figure 1.31, but before removal of endocardium and valve leaflets The commissure of the septal and anterosuperior leaflets of the tricuspid valve lies adjacent to the centre of the field marking the position of the membranous septum. The orifice of the coronary sinys is visible to the left and immediately above it a fold of tissue representing the eustachian valve. The prolongation of the fold towards the membranous septum Is the tendon of Todaro. The triangle of Koch is delimited by the mouth of the coronary sinus, the tendon of Todaro and the septal attachment of the tricuspid valve. Within it lies the AV node. If one views Figure 1.31, it is evident that the node is not visible to the naked eye.

axis of the heart) (Figure 1.35). The pulmonary valve sits anteriorly and to the left of the aortic valve and at an angle of approximately 45 degrees to it. Both arterial valves have three cusps with associated commissures (Figure 1.36). Each valve cusp has a semicircular attachment to the ventriculoarterial junction with the convex aspect on the ventricular side. The free edges meet at the commissures on the arterial aspect. The pocket thus formed between each cusp and the arterial
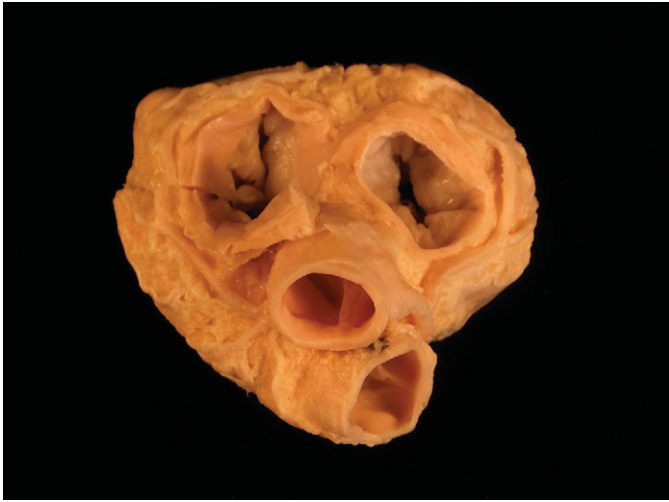
Figure 1.35 Dissection of heart to demonstrate the relations of the great arteries. The heart is viewed from above with the posterior aspect at the upper part of the field and the anterior aspect on the lower part. The right ventricle is to the left of the field and the left ventricle to the right. The aorta sits in the centre of the base of the heart and the pulmonary trunk is anterior to it and to the left. The aorta is wedged between the two atrioventricular valves. The axes of the two great arteries are at an angel of approximately 45 degrees to each other. It can be appreciated that the commissure of the two valvar cusps in the anterior aorta abuts the commissure of the two posterior cusps in the pulmonary trunk. The origins of the coronary arteries from the facing sinuses of the aortic valve are also evident, as is the way that the right ventricle is wrapped around the anterior aspect of the left.

Figure 1.36 Normal pulmonary valve. The right ventricular outflow tract has been opened to expose the pulmonary valve. The circumference of the valve contains three cusps that have a semicircular attachment to the ventriculoarterial junction. They are attached such that the lower part of the sinus of each overlies myocardium while the upper part of the sinus overlies arterial wall. Similarly, on the ventricular aspect of each cusp, part of the triangular space between the cusps overlies arterial wall and the remainder overlies myocardium. The aortic valve where it is attached to the ventricular wall has a similar arrangement. The free edges of the cusps also have a semicircular profile when viewed from the arterial side. When closed, the three cusps come together to give a triradiate appearance. The line of apposition of the cusps is not in fact at the free edge but slightly lower on the cusp.

wall is termed a sinus. The artery at the site of the valve bulges outward slightly such that when the valve is fully open, the cusps fill the recess and do not impair the forwards flow of blood from the ventricle to the artery. The line of apposition of the cusps when the valve is closed lies not at the free edges of the cusps but a little way below this. The area between the free edge and the line of apposition is called the lunula. A small nodular area of thickening is present in the centre of the free edge of each cusp – the nodule of Arantius (Figure 1.37).

The commissure of two of the cusps of the pulmonary valve is contiguous with the commissure of two of the cusps of the aortic valve to produce facing sinuses in each valve (Figure 1.35). The two facing sinuses of the aortic valve give rise to the coronary arteries. The pulmonary valve is supported by a complete muscular infundibulum (Figure 1.22); the aortic valve, by contrast, has a rim supported only partly by muscle and partly by the fibrous continuity between the left coronary and non-coronary leaflets of the aortic valve and the anterior leaflet of the mitral valve (Figure 1.26). A muscle bundle, the "anterolateral muscle bundle of Moulaert", is conspicuous in about 40% of hearts (Figure 1.38) [14].

The aorta and pulmonary trunk have a spiral relationship to each other – the pulmonary trunk extending backwards and to the right and the aorta slightly forwards and to the left (Figure 1.39). In the fetus and neonate the arterial duct is a direct continuation of the pulmonary trunk to the descending thoracic aorta with a narrow angle between its superior surface and the aortic arch (Figure 1.40). Later growth of the pulmonary
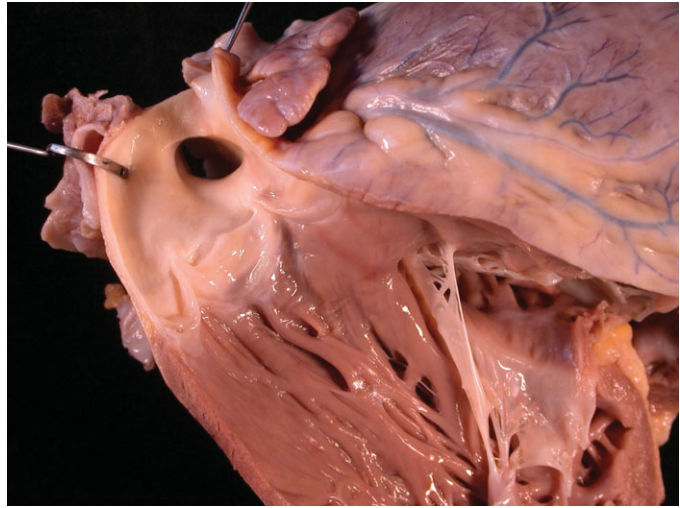

Figure 1.37 Semilunar valve cusp morphology. Excised aortic valve cusps. Each is semilunar in shape. The free edge shows a slight nodular thickening in its mid part – the nodule of Arantius. Between the free edge of the cusps and the line of apposition, the valvar tissue is thin and, frequently, as here, fenestrated.

artery and aorta causes the angle between the duct and the aorta to approach at more of a right angle (Figure 1.41).

1.2.9 Coronary Arteries

The coronary arteries arise from the right- and left-facing sinuses of the aortic valve. Although Anderson and co-workers

Figure 1.38 Anterolateral muscle bundle of Moulaert. Left ventricular outflow tract opened by bisecting the anterosuperior leaflet of the mitral valve. The cut end of the mitral valve is grasped in the forceps. Extending from the area of the left fibrous trigone, a prominent muscle bundle descends between the septum and the ventricular wall. This feature is said to occur in up to 40% of normal hearts, but its prominence is very variable. While it has the potential to narrow the outflow tract, of itself it does not cause problems.
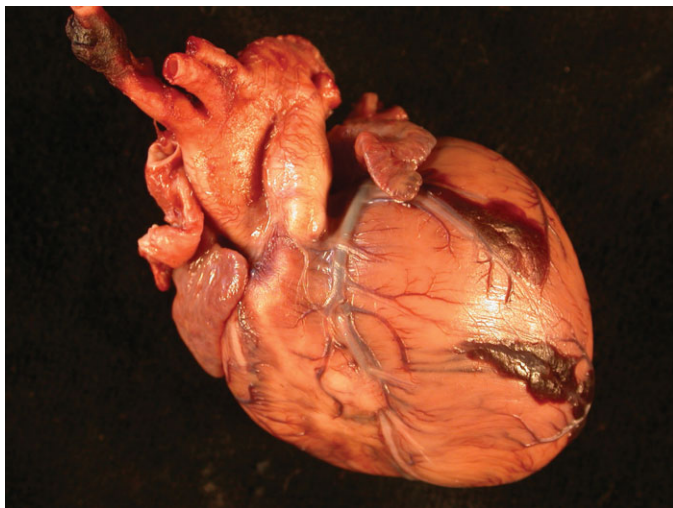

Figure 1.39 Spiral relation of aorta and pulmonary artery. Normal fetal heart at 22 weeks' gestation. The rightward spiral of aorta and pulmonary artery around each other is well seen.
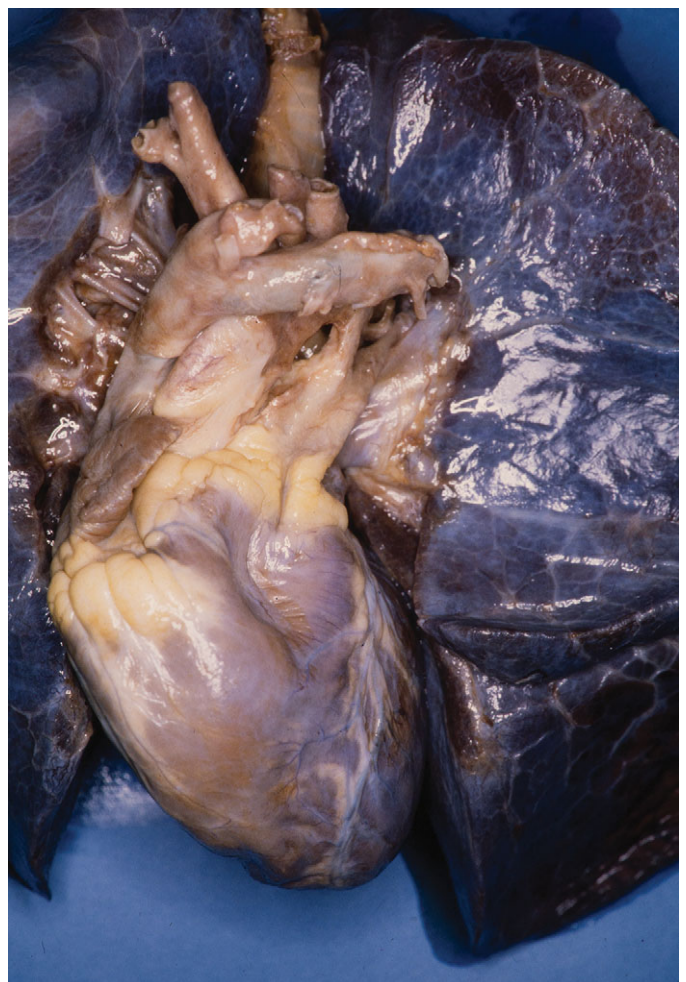

Figure 1.40 Neonatal arterial duct in a one-day-old infant. The arterial duct is evident as an upwards continuation of the pulmonary artery. It joins the inferior aspect of the aortic arch at an acute angle.

have urged the naming of the sinuses as 1 and 2 (as viewed from a hypothetical observer sitting in the non-coronary sinus and observing the sinus at their right hand as number 1 and that at their left hand as number 2), this is at variance with their otherwise stated preference for avoidance of alphanumerical systems of classification [15]. They arise from within the valve sinus and below, or sometimes at the level of the sino-tubular junction. The left artery arises from the left-facing sinus, and there is usually only one orifice. The right artery arises from the right-facing sinus. In up to 50% of normal hearts there is a second, smaller orifice giving rise to an

Figure 1.41 Post-neonatal arterial duct. The angle of entry of the arterial ligament into the pulmonary arterial wall is greater than in the neonate.

Figure 1.42 Multiple right coronary artery orifices. The left ventricular outflow and aortic valve opened to demonstrate the coronary artery orifices. To the left of the field the left coronary artery arises via a single orifice from the left sinus of Valsalva. In the centre the right coronary artery arteries from the right sinus of Valsalva . There are three orifices. The main orifice is towards the commissure with the non-coronary cusp. Two smaller orifices are visible towards the centre of the sinus, representing the orifices of infundibular branches.

infundibular (conus) artery (Figure 1.42) [16]. The orifices are usually in the central part of the sinus, but they may be located close to the commissures. The epicardial course of the coronary arteries is in the atrioventricular grooves and the interventricular grooves. In about 90% of subjects the posterior (inferior) interventricular coronary artery takes origin from the right coronary artery – so-called right-dominance (Figure 1.43). In most of the remainder the posterior interventricular artery has its origin for the left circumflex artery, so-called left dominance (Figure 1.44). In a small number of cases there are posterior interventricular arteries arising from both right and left circulations, the so-called balanced pattern (Figure 1.45).

An exceptionally rare occurrence is the origin of the left coronary artery from the posterior sinus [17].

The right coronary artery emerges directly from the aorta into the adipose tissue of the right atrioventricular groove and overlies the supraventricular crest. It courses in the groove around the tricuspid valve to supply the inferior surface of the heart. If the infundibular artery does not arise directly from the sinus, it forms one of the first branches of the right coronary artery after its exit from the aorta. The sinoatrial node branch is also an early branch in about 50% of cases (in the remainder, this artery arises from the early part of the course of the left circumflex artery) (Figure 1.46). The next major branch of the right coronary artery is the marginal branch running towards the apex on the acute margin of the heart. In those hearts with right-dominance, the posterior interventricular artery from the right coronary artery supplies the inferior wall of the left ventricle and the posteromedial papillary muscle of the mitral valve.

Figure 1.43 Right dominant coronary circulation. The normal heart viewed from its diaphragmatic surface. The right coronary artery can be seen at the top centre of the field as it courses in the right atrioventricular groove from the anterior surface of the heart. Adjacent to the inferior caval vein it gives off a posterior descending artery that travels towards the apex, together with the middle cardiac vein. The circumflex artery is seen at the bottom of the field in the left atrioventricular groove as it terminates in a branch running obliquely over the diaphragmatic surface towards the apex. The posterior vein of the left ventricle runs from the atrioventricular groove towards the apex equidistant from the two arteries.

The left coronary artery has a short undivided course following its exit from the aorta. It divides to the left of the pulmonary artery to form anterior descending (interventricular) and circumflex branches. In about one-third of individuals a third vessel arises at this branching point, called the first diagonal branch (or intermediate artery) that courses obliquely over the anterolateral wall of the left ventricle (Figure 1.47). The anterior descending artery gives off diagonal branches supplying the obtuse margin of the heart. It also gives off perforating branches into the interventricular septum. In many cases the left anterior descending coronary artery has a short intramyocardial course before re-emerging onto the epicardium (Figure 1.48).

The circumflex artery has a variable course depending on whether or not there is right-dominance. The artery to the AV node arises from the dominant coronary artery at the crux of the heart (junction of the interatrial and atrioventricular grooves inferiorly) (Figure 1.49) [18].

1.2.10 Cardiac Veins

The veins of the heart are usually ignored by pathologists, seen, if seen at all, as a minor inconvenience in dissecting the coronary arteries. There has been renewed interest in their anatomy of late because of their usefulness in cardiac catheterisation and electrophysiological studies [19]. Most of the cardiac venous return is via epicardial veins to the coronary sinus (Figure 1.50) [20]. The major named veins are:

1. The **great cardiac vein**. It originates at the cardiac apex and ascends on the anterior surface of the epicardium in the

Figure 1.44 Left-dominance coronary artery. The heart is viewed from below and behind. In the upper centre of the fields is the right atrial appendage with the inferior caval vein orifice to its left. The left atrial appendage is visible in the left centre. The atrioventricular groove runs horizontally in the field and within it, from the left side, is the circumflex artery. The artery turns and descends towards the apex at the crux of the heart, forming the posterior interventricular artery.

Figure 1.45 Balanced coronary circulation. An explanted heart from a ten-year-old girl viewed from behind following dissection of the coronary arteries. The right coronary artery and the left circumflex artery both reach the crux of the heart where they both supply a descending artery.

Figure 1.46 Proximal right coronary artery. Heart viewed from anteriorly. The pulmonary infundibulum is retracted to the left to expose the origin of the right coronary artery from the aorta. At least five branches run from the artery to the right of the field, supplying the anterior right ventricular wall and pulmonary infundibulum. A large branch runs between the right atrial appendage and the aorta, ascending on the medial aspect of the right atrium towards the junction with the superior caval vein. This is the artery to the sinoatrial node.

anterior interventricular groove to reach the left atrioventricular sulcus where it turns leftwards and travels around the obtuse margin of the heart where it is continuous with the coronary sinus, the entry of the vein of Marshall marking the junction. Its major tributary is the left (obtuse) marginal vein, which is present in over 80% of people.

2. The **middle cardiac vein**, which runs in the posterior interventricular groove and enters the coronary sinus near its orifice. In the majority of hearts with right coronary artery dominance, it is in close proximity to the right coronary artery.

3. The **small cardiac vein**, sometimes referred to as the right cardiac vein, which runs in the right atrioventricular groove and joins the coronary sinus near its orifice.
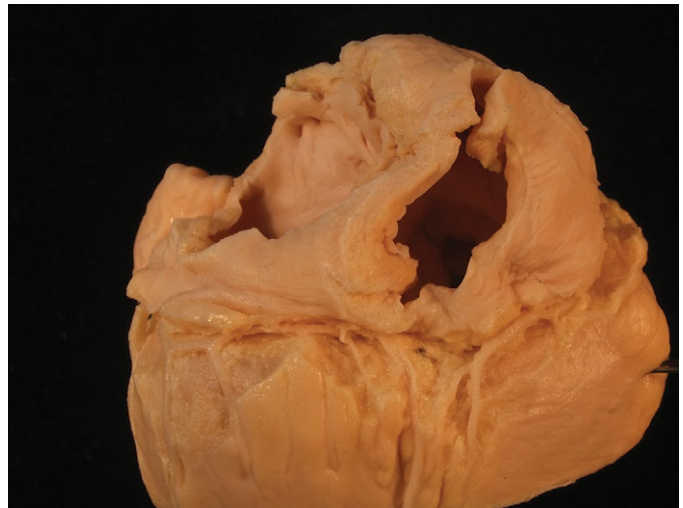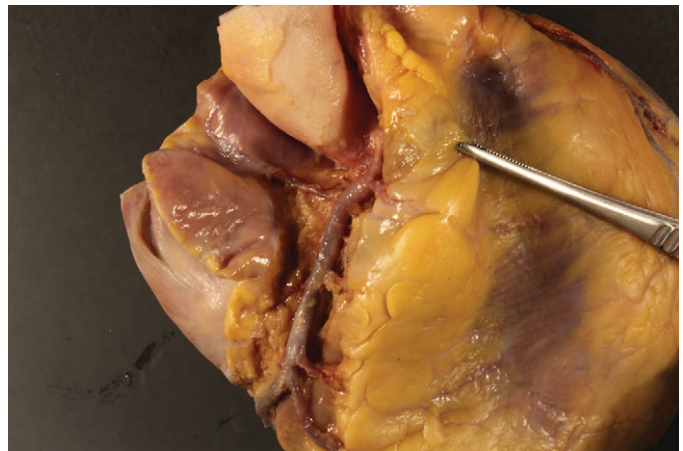
4. The **posterior vein of the left ventricle**, which runs on the left ventricle's diaphragmatic surface to the left of the middle cardiac vein. It is only identifiable in about 50% of hearts.

5. The **oblique vein of the left atrium**, which is a remnant of the left superior caval vein and may persist. It runs obliquely along the posterior aspect of the left atrium and joins the coronary sinus, marking its junction with the great cardiac vein.

6. The **right (acute) marginal vein** may open directly into the right atrium or sometimes into the small cardiac vein.

There is considerable crossing of veins over arteries and arteries over veins at the obtuse margin of the heart (circumflex
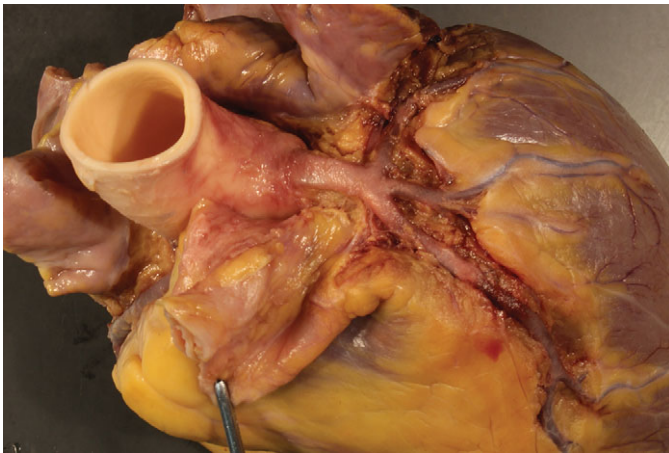
Figure 1.47 Left coronary artery and intermediate branch. The heart is viewed from the left anterior position. The left coronary artery has been dissected from its origin from the aorta. The pulmonary trunk has been drawn forwards and to the right to expose the full course of the artery. The short main stem divides into three. Superiorly the circumflex artery runs in the left atrioventricular groove beneath the left atrial appendage. The anterior descending artery crosses the field obliquely to the lower right field. Between these two arteries a third artery arises – the intermediate artery.
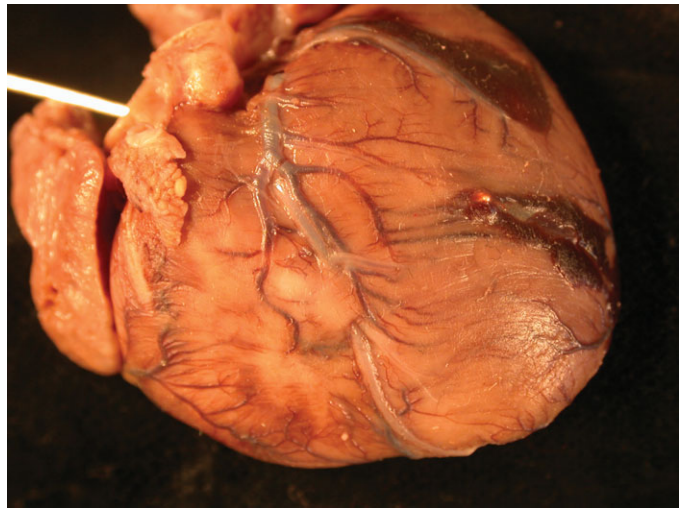

Figure 1.48 Intramyocardial course of left anterior interventricular artery. A six-day-old infant with pulmonary atresia. The epicardial surface of the left ventricle shows very distended veins. In addition, there is a short segment of the left anterior descending artery that is not present on the surface but dips into the myocardium before resurfacing further distally. This is of no significance.

Figure 1.49 Atrioventricular nodal artery. Heart viewed from inferiorly following dissection of the coronary arteries. There is right dominant circulation with the right coronary artery supplying the posterior interventricular artery. From the point where the right coronary artery leaves the atrioventricular groove to descend in the interventricular groove arises a smaller branch that enters the myocardium at the crux – the artery to the AV node. This artery usually arises from the dominant artery. The vessel forming the third side of a vascular triangle in this dissection is the middle cardiac vein that ascends to enter the coronary sinus to the left of the atrioventricular nodal artery.

Figure 1.50 Cardiac veins. The posterior atrioventricular junction in this heart has been dissected to demonstrate the cardiac veins. The coronary sinus occupies the greater part of the posterior atrioventricular junction. Branches on the epicardium of atria and ventricles join it.

For a review of the literature on cardiac veins, see reference [20].

Several veins do not drain to the coronary sinus; the anterior cardiac veins run over the front of the right ventricle and open directly into the right atrium crossing over the course of the right coronary artery in the right atrioventricular groove. In up to a quarter of cases they may merge to form a common trunk before entering the right atrium [21]. The right ventricle and both atria are drained by these veins. Small veins in the atrial, and sometimes the ventricular, walls may open directly into the adjacent cavity.

The epicardial veins drain the external two-thirds of the myocardium. The inner one-third is drained by veins directly into the luminal chambers. These are termed thebesian veins [19].

artery) and at the crux (right coronary artery) [21]. The veins contain valves. The most prominent is the thebesian valve at the mouth of the coronary sinus (Figure 1.13). Within the coronary sinus at its junction with the great cardiac vein and oblique vein of the left atrium (vein of Marshall) is another named valve – the valve of Vieussens. The coronary sinus has a sleeve of myocardium from the left atrium.
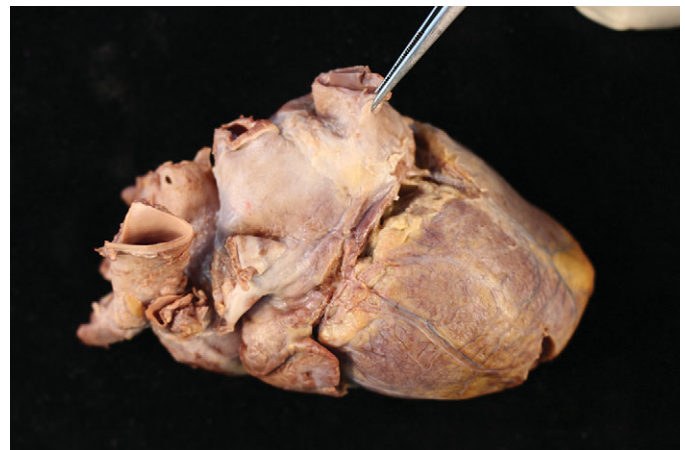
1.3 Histology

1.3.1 Pericardium

The pericardium consists of a layer of collagenous fibrous tissue with blood vessels. The surface facing the pericardial cavity is lined by a single layer of mesothelial cells. Focally there may be epicardial extra-medullary haematopoiesis around the origins of the great arteries and coronary arteries (Figure 1.51). Brown fat can occur in the epicardium even into the teen years. Epicardial fat extends into the apparent interatrial septum. Fat cells are also present along the course of the intramyocardial coronary arteries and may be prominent, particularly on the right side (Figure 1.52).
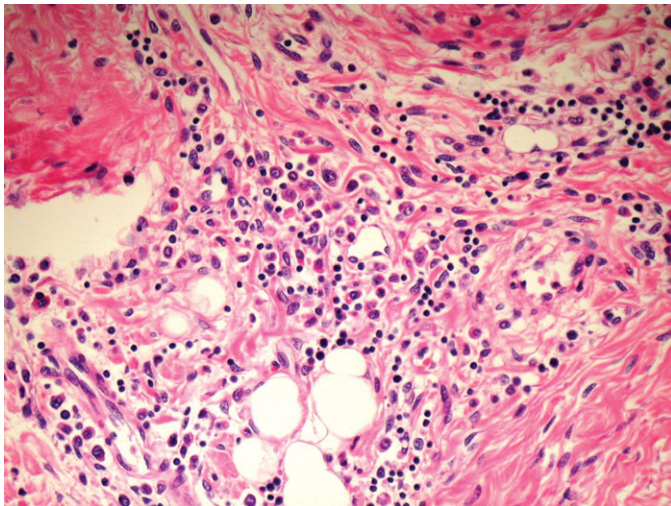
1.3.2 Myocardium

The myocardium is made up of individual myocytes. Cardiomyocytes account for about 80% of the volume of the heart, but as a proportion of cells present they represent only about 30% [22], the remainder being composed of endothelial cells, fibroblasts and smooth muscle cells [23]. The myocardium has the structure of a modified blood vessel with the individual myocytes arranged tangentially and, in some cases, obliquely in the wall but with distinct anatomical units. The general orientation of the myocytes varies at different depths within the myocardium [24]. Histologically, the fetal myocardium appears more vacuolated than its adult counterpart (Figure 1.53). Mitotic figures may be seen up to the time of birth and probably also for a short while thereafter in the neonatal period (Figure 1.54).
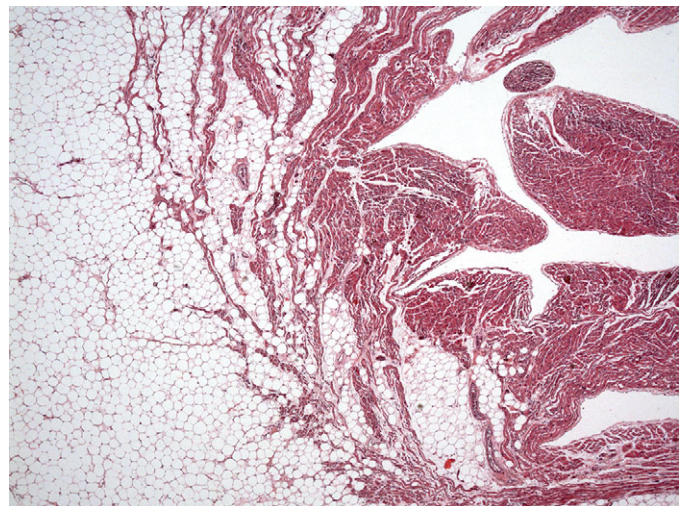

Figure 1.51 Extramedullary haemopoiesis of epicardium. Sudden death aged 1 month. The epicardial surface of the heart shows a small focus of extramedullary haemopoiesis. Erythroblasts and myeloblasts are present admixed with the epicardial fat.

Figure 1.52 Fat in the right ventricular myocardium. Adolescent female who died of non-cardiac causes. A section from close to the right ventricular apex showing extensive fatty infiltration, almost to the endocardium. Critically, there is no associated fibrosis.
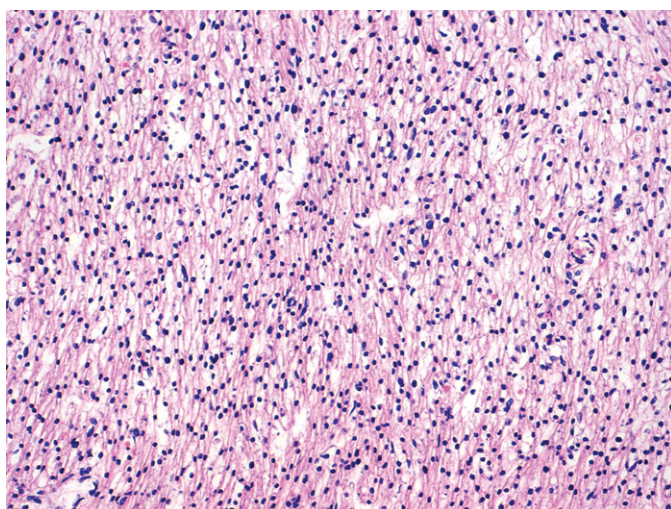

Figure 1.53 Fetal myocardium. Section of myocardium of a fetus of 20 weeks' gestation. The myocytes are thin and closely packed and the nuclei appear crowded. The nuclei are relatively hyperchromatic and the cytoplasm slightly vacuolated.
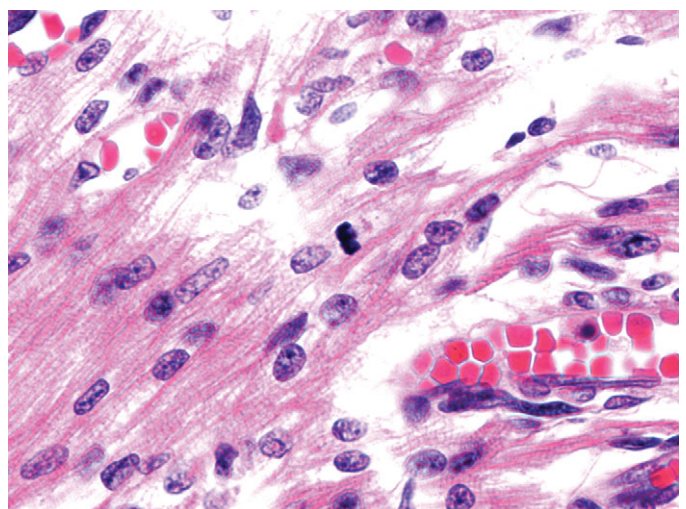

Figure 1.54 Mitotic figures in myocardium. Ventricular myocardium in an 18-week fetus. In the centre of the field is a mitotic figure within a myocyte. Such mitotic figures can be found in normal hearts up to term and in post-neonatal diseased hearts where they may represent failure of the normal switching off mechanism.
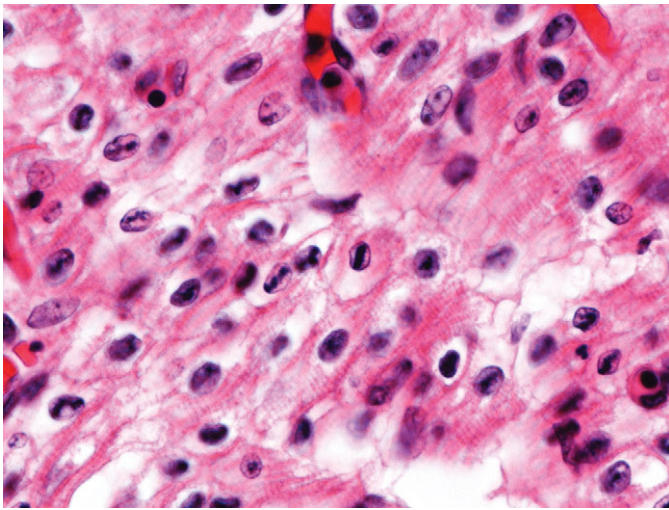
Figure 1.55 Anitschkow cells. Female infant born at 29 weeks' gestation with dilated cardiomyopathy and hydrops. She died aged 3 days. In a high-power view of the ventricular myocardium, at least five myocyte nuclei are visible that show clearing of the nucleus and a longitudinal bar of dark chromatin. Several nuclei are cut in their short axis where the chomatin is visible as a central bullseye.
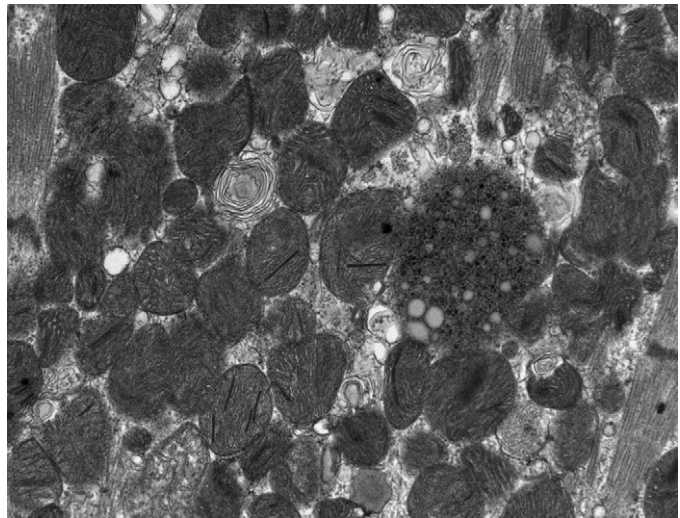

Figure 1.56 Lipofuscin myocytes (child). Among the numerous mitochondria present there is a rounded structure composed of granular osmiophilic material with included small lipid droplets. This is the characteristic feature of lipofuscin. Although not obvious in this example, lipofuscin is membrane bound in lysosomes (Figure courtesy of Mr G. Anderson, Clinical Electron-microscopist, Great Ormond Street Hospital, London).
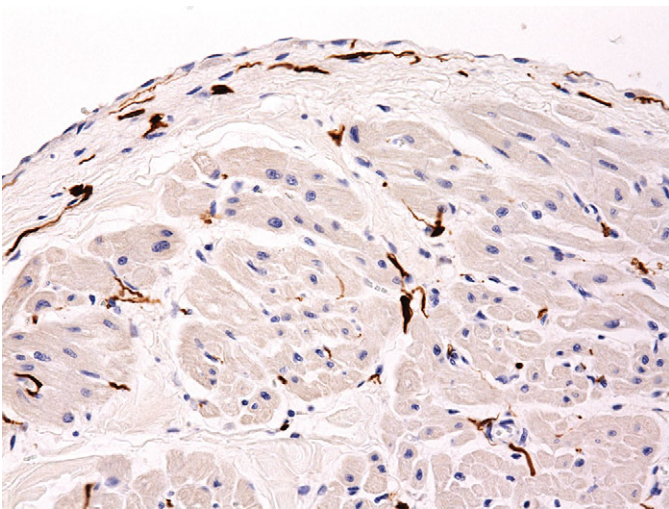

Figure 1.57 Nerves in a normal heart. A section from the right ventricular myocardium of a four-year-old stained with antibody S100. Between the myocytes there are numerous fine nerve twigs, many associated with small vessels. There are also numerous fine nerve fibres in the endocardium.
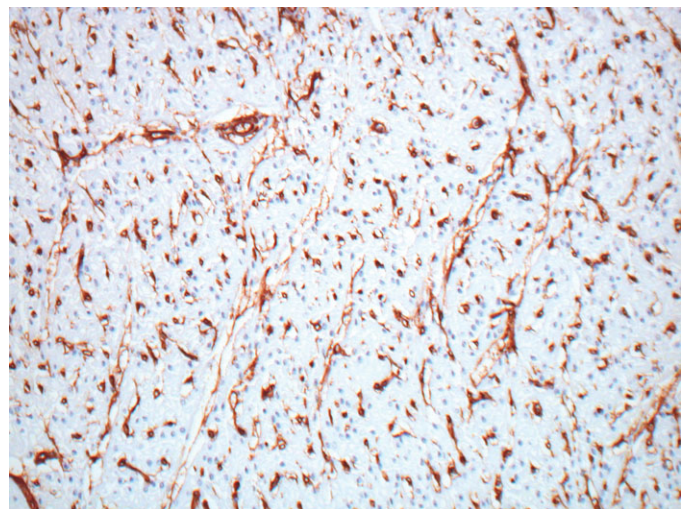

Figure 1.58 Capillaries of the heart. Section of normal myocardium stained with antibody to CD34 to demonstrate the density of the capillary network within the myocardium.

Myocyte nuclei may show Anitschkow nuclear features [25]. This consists of a central solid bar of chromatin in longitudinally cut nuclei with surrounding clear nucleoplasm (Figure 1.55). In cross section these nuclei have an owl-eye appearance. Similar nuclear features may be present also in interstitial cells (including macrophages) and Schwann cells, and in valvar stromal cells [26]. The phenotype seems largely confined to the heart in the fetus and infant, although occasional foci of such nuclei may be seen in the larynx. The significance if any of this change is unknown. Neonatal cardiac myocytes do not contain lipofuscin pigment; this first becomes recognisable on light microscopy at about nine years of age [27], although it may be seen on electron microscopy earlier (Figure 1.56).

In contrast to skeletal muscle, which is composed of very long fibres that result from the progressive fusion of hundreds of cells during embryogenesis, and in which each cell is supplied by a nerve fibre and contracts individually in response to stimulation through its own neuromuscular junction, the cardiac myocytes form a syncytium linked by intercalated discs. Nerve fibres, especially of the autonomic variety, are found throughout the heart (Figure 1.57), but they do not serve the purpose of stimulating the muscle cells to contract. Rather, they seem to regulate the overall activity of the heart. The normal myocardium is an extremely vascular structure and staining for endothelial cells reveals just how vascular it is (Figure 1.58).
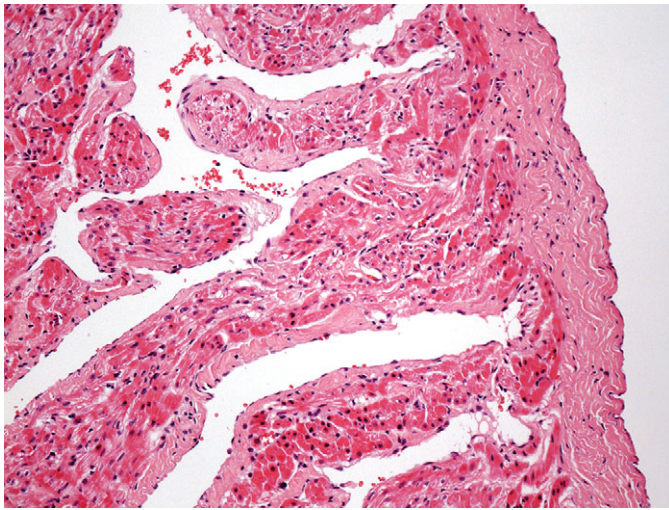
Figure 1.59 Right atrial myocardium. There are deep recesses in the wall where the myocardium is excluded and the endocardium rests on the epicardium.
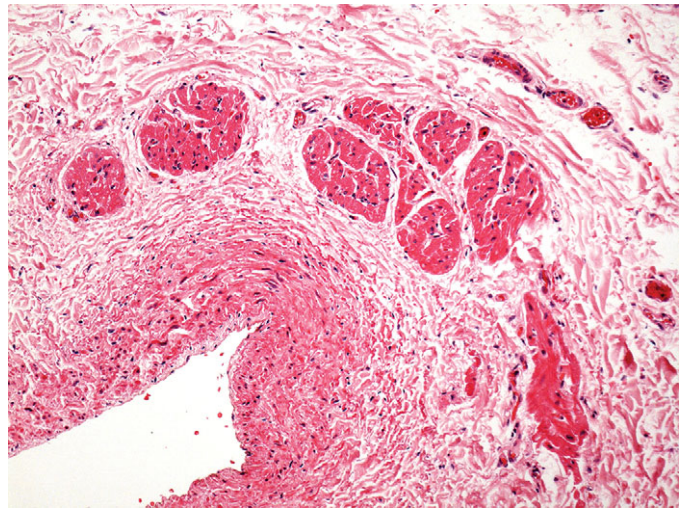

Figure 1.60 Myocardium around pulmonary veins. Myocardium in adventitia of pulmonary veins. Sixteen-month-old female with DiGeorge syndrome. Sudden death.
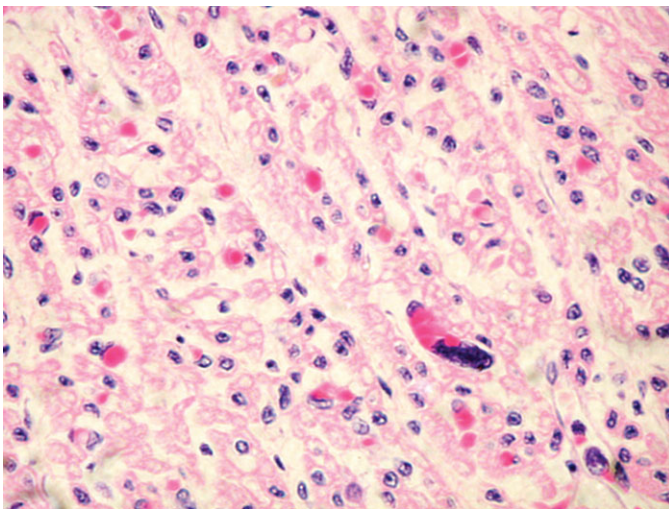

Figure 1.61 Megakaryocytes. High-power view of the myocardium from a patient who had dilated cardiomyopathy. There is intense capillary congestion with many of the capillaries containing erythrocytes. In the centre of the field a large irregular nucleus is present within a distended capillary. This represents a megakaryocyte nucleus.
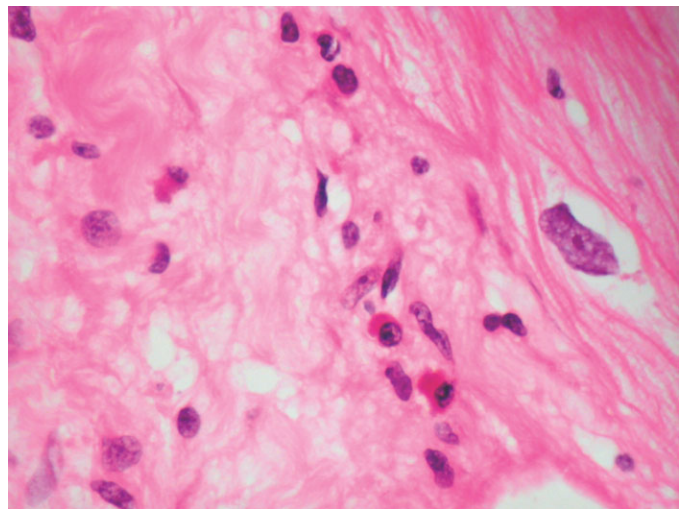

Figure 1.62 Mast cells in a normal heart. High-power view of the myocardium shows an area of fibrous tissue that contains mast cells. The cells have rounded nuclei that are eccentric and show coarse chromatin; the cytoplasm is opaque and pinkish purple. At least three mast cells are present in this field.

The myocardium of the right atrium is composed of muscular trabeculations. Between the trabeculations the wall can be quite thin and, in places, the endocardium rests directly on the pericardium without intervention of cardiac muscle (Figure 1.59).

Small amounts of atrial myocardium may extend into the pulmonary veins external to the muscular media (Figure 1.60) [28]. Megakaryocytes, or at least their nuclei, may occasionally be seen within capillaries in the myocardium (Figure 1.61). It has long been known that they occur in adult myocardium in about 16% of cases of traumatic sudden death and in 45% of cases of hospital deaths [29].

Mast cells are a component of the interstitium of the normal myocardium. Their numbers are increased in myocarditis and dilated cardiomyopathy and, indeed, in any condition that induces an increase in cardiac fibrous tissue (Figure 1.62) [30].

1.3.3 Endocardium

The endocardial layer of the left atrium is thicker than that of the right (Figure 1.63). The epicardium and endocardium come very close together in the atrial appendages and between the pectinate muscles (Figure 1.59); in the neonate, fluid under pressure in central lines may leak into the pericardial space in these areas. The atrial endocardium, and sometimes the ventricular endocardium, contains smooth muscle cells (Figure 1.64), and sometimes these can be quite prominent.
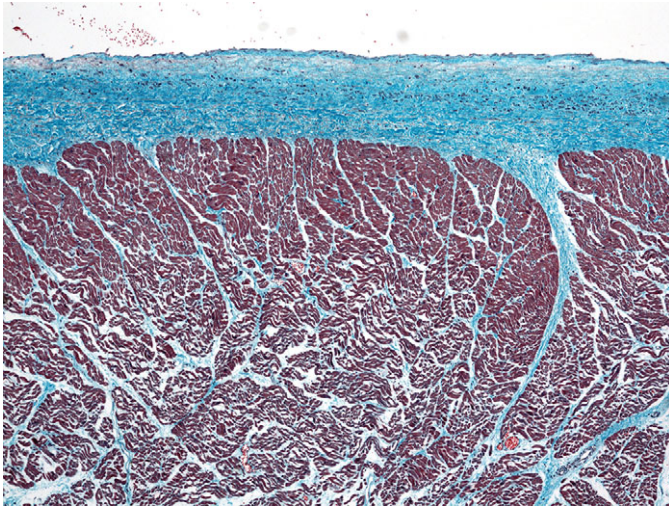
Figure 1.63 Endocardium of left atrium. A Masson's trichrome stained section of normal left atrium showing the thick endocardium of this chamber. It should not be mistaken for a pathological process.
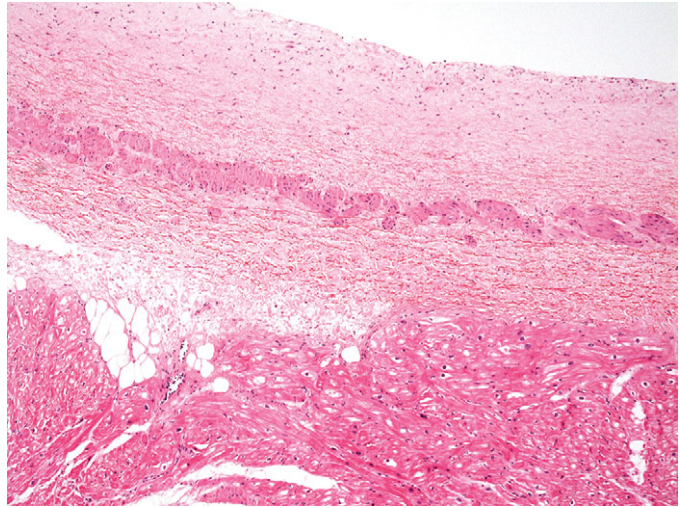

Figure 1.64 Smooth muscle atrial endocardium. A case of hypertrophic cardiomyopathy. This section of the left atrium endocardium shows a continuous sheet of smooth muscle cells within the thickened endocardium.
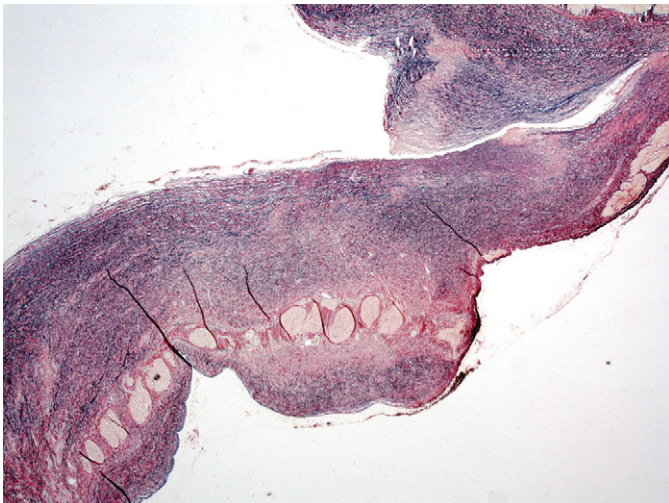

Figure 1.65 Histology flap valve of oval fossa. This specimen is from a heart explanted from a neonate with cardiomyopathy and is stained with Elastic vanGieson. The right atrium is above, and the left below the flap valve consists of an irregular layer of fibroelastic tissue in which there are discontinuous bundles of myocardium. The point of attachment to the left atrium is seen to the right upper part of the field. On the right atrial side of the valve there is deposition of laminar elastic tissue over the attachment point.

Figure 1.66 Prichard's structures. A two-month old-girl with a structurally normal heart who died of sepsis. A high-power section through the flap valve of the oval fossa shows small clusters of cells with dark nuclei and scanty cytoplasm. These represent endothelial structures commonly seen in this area – so-called Prichard's structures.

The interatrial septum, more particularly the flap valve of the oval fossa, is a muscular structure (Figure 1.65). In the endocardium on both right and left sides there are clusters of cells with hyperchromatic nuclei resembling multinucleate cells [31]. These cell clusters have received little attention in the literature but appear to be of endothelial origin [32] (Figure 1.66).

The endocardium has a limited repertoire of response to injury, and this response usually assumes the form of fibroelastic thickening. The intimal surfaces of the valves, which are essentially endocardium, also exhibit a similar response to injury, and a similar reaction is seen in the intima of the great arteries. Thus, in endocardial fibroelastosis, in valvar stenosis and damage, and in the intimal proliferation in response to vessel injury or in the intima of grafts, a very similar picture is seen of layered fibroelastic thickening with variable cellularity. The younger the tissue, the more likely it is to be cellular. Inflammatory cells, while they may occasionally be found, are not a prominent component of the response.

1.3.4 Valves

The atrioventricular and arterial (semilunar) valves have a similar histological structure. The atrioventricular valves are slightly thicker than the arterial valves and the left-sided valves

Figure 1.67 Histology of normal atrioventricular valve.

Figure 1.68 Histology of normal ventriculoarterial (semilunar) valve.

slightly thicker than the right-sided ones [33]. They have a dense collagenous layer – the fibrosa that extends from the base to t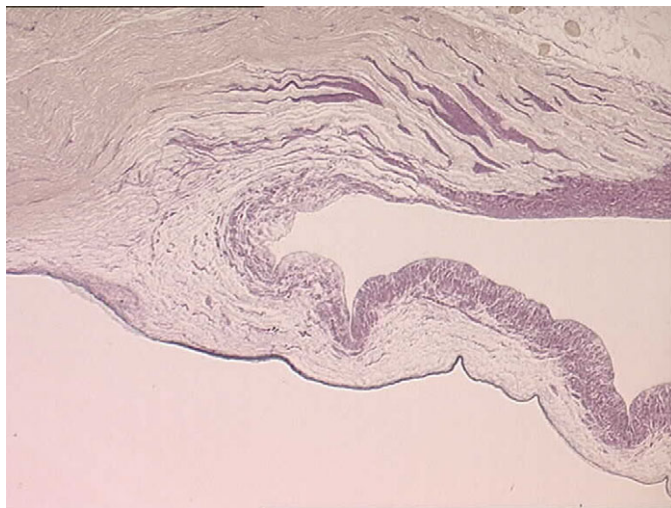he free edge with the collagen bundles circumferentially arranged. In the arterial valves there is a layer termed the ventricularis and in the atrioventricular valves an equivalent layer termed the atrialis composed of radially oriented elastic fibres lying beneath the endocardium. The ventricularis/atrialis does not extend to the free edge of the valve. In the atrioventricular valves the fibrosa lies on the ventricular aspect, while in the arterial valves the fibrosa is on the arterial aspect. This permits orientation even of excised valvar leaflets – the side of the valve exposed to the higher cavity pressure (the ventricular aspect of the AV valves and the arterial aspect of the arterial valves). Lying between these two layers is the spongiosa composed predominantly of proteoglycans (Figures 1.67 and 1.68). The spongiosa does not extend to the free edge of the valve leaflet. Covering the surface of the valve is a thin layer of endothelium. The valves are more cellular in the child than in the adult and may be rather myxoid, but should not be nodular. If nodular and myxoid, then they are considered dysplastic (Figure 1.69). Calcification may occur in degenerate valves, and cartilage is reported in some and sometimes even woven bone [34].

Blood cysts (Figure 1.70) are a very frequent finding. These are rounded nodules filled with blood, usually on the atrioventricular valves, although they may sometimes be seen on the arterial valves. They lie near the line of closure on the atrial aspect of the atrioventricular valves or towards the base of the ventricular aspect of the arterial valves. Histologically, they are rounded, blood-filled spaces lined by endothelium [35]. They may be multilocular and are frequently multiple (Figure 1.71). They may measure up to 3 mm in diameter, but many are smaller. There may be haemosiderin in the surrounding valvar stroma. They usually disappear by about six months of age. They may, however, persist and form giant blood cysts [36].

Figure 1.69 Dysplastic valve. Excised dysplastic mitral valve leaflets from a 10-year-old with Robinow's syndrome. The leaflets are thickened and nodular, and the chordae are thickened and partly fused.

There is no consensus as to their origin, and multiple hypotheses have been proposed to explain their development:

- They are formed during valve development as a result of blood trapped in crevices that later seal off.
- They are the result of haematomas secondary to the occlusion of small vascular branches of end arteries.
- They result from metaplastic change in the tissue that comes from primitive pericardial mesothelium.
- They represent ectatic or dilated blood vessels in the valve.
- They are simple angiomas.

They are of no significance except in the very rare instances where they develop into giant cysts and obstruct the flow of blood [37].
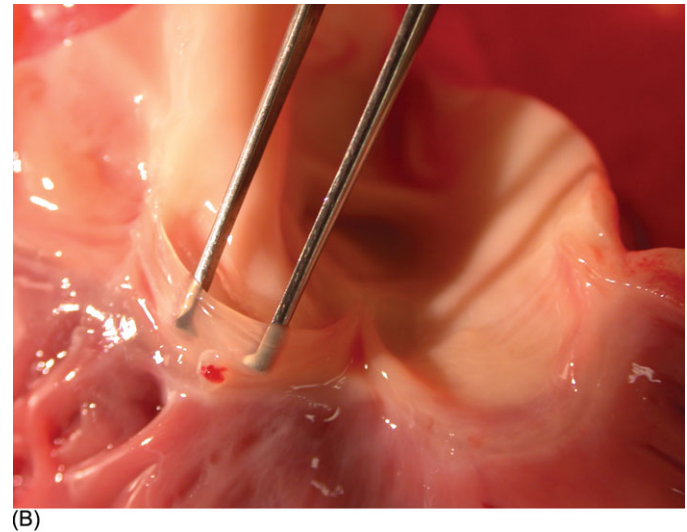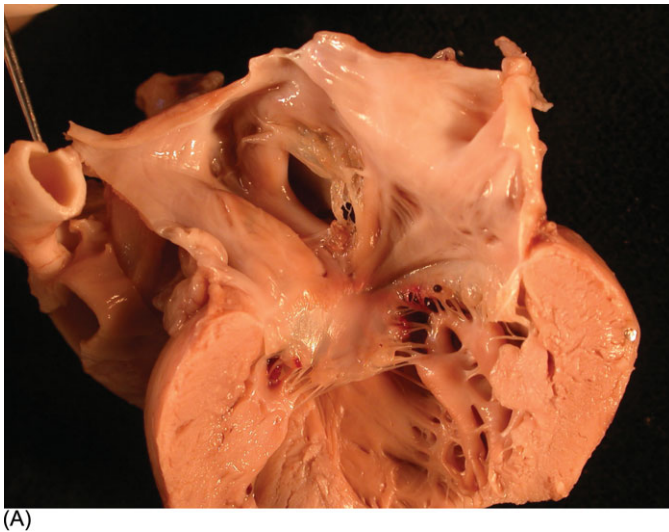
Figure 1.70 **(A)** Blood cyst atrioventricular valve. Eight-week-old male infant. The left side of normal heart opened to show blood cysts on the mitral valve. The cysts are visible as black nodules adjacent to the free edges of the mural leaflet of the valve. A secundum atrial septal defect is also visible. **(B)** Blood cyst semilunar valve. A small blood cyst is present on the ventricular aspect of one of the cusps of the pulmonary valve. A pair of forceps has been inserted into the sinus to distend the cusp, which shows a partially blood-filled cyst protruding from the ventricular aspect adjacent to the point of attachment to the ventricle.
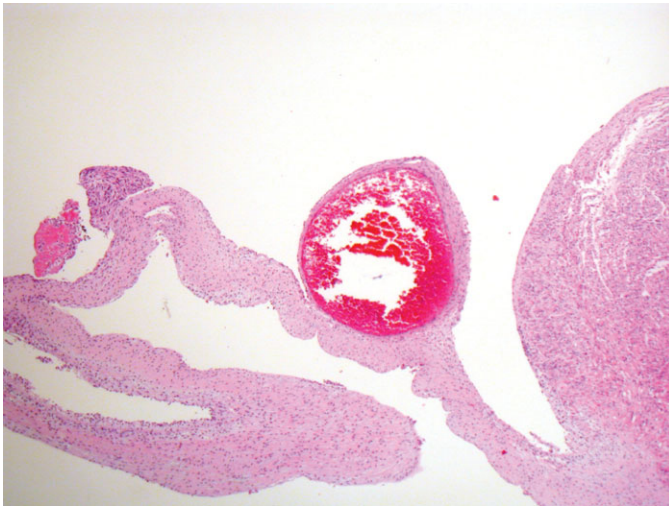

Figure 1.71 Blood cyst – microscopic appearance. Three-week-old female infant. The sections show an atrioventricular valve with a blood cyst protruding from the atrial surface. The cyst is lined by flattened endothelial cells, contains fresh blood and there is a compressed thin fibrous wall.

1.3.5 Conduction Tissue

The sinoatrial node, the pacemaker of the heart, is situated at the junction of the superior caval vein and the crest of the right atrial appendage. In approximately 10% of individuals the node straddles the apex of the junction and extends into the interatrial groove [38]. It lies beneath the epicardium. Histologically, it comprises a triangular area of myocardium, the constituent cells of which are smaller than the surrounding "working" atrial myocardium, but which at the periphery of the node intermix with the atrial myocardium (Figure 1.72A). A very helpful marker of its site is the central large sinoatrial nodal artery [10]. There is also a close association with branches of the vagus nerve. With increasing age, there is increase in interstitial fibrous tissue. The nodal cells stain positively for smooth muscle actin, in contrast to the surrounding myocardium and the cells of the AV node, which are negative (Figure 1.72B).

The AV node is situated in the right atrium in the triangle of Koch, above the atrioventricular junction and lying between the mouth of the coronary sinus and the membranous septum. Histologically it is a pyramidal area of myocytes lying beneath the endocardium and a thin layer of atrial myocardium and abutting the fibrous tissue of the central fibrous body (the membranous septum and the rightward extension of the mitral aortic fibrous continuity) (Figure 1.73). Transitional cells connect it to the atrial working myocardium. Tissue from the node extends as the bundle of His superiorly into this fibrous tissue, which insulates it from the myocardium. Within the membranous septum it lies on the apex of the muscular component of the interventricular septum and branches to give left and right bundle branches (Figure 1.74). The left branches lie immediately beneath the endocardium of the left ventricular outflow tract and consist of several thin bands of tissue that fan out beneath the endocardium to connect with the Purkinje cells. The right bundle branch, by contrast, remains as a single cord of cells and lies deep within the myocardium of the septomarginal trabeculation before entering the moderator band and reaching the parietal wall of the right ventricle.

1.3.6 Coronary Arteries

The coronary arteries have the structure of muscular systemic arteries with a well-developed muscular tunica media separated from a thin tunica intima by a well-developed internal elastic lamina. The outer aspect of the tunica media is separated from the tunica adventitia by an incomplete layer of
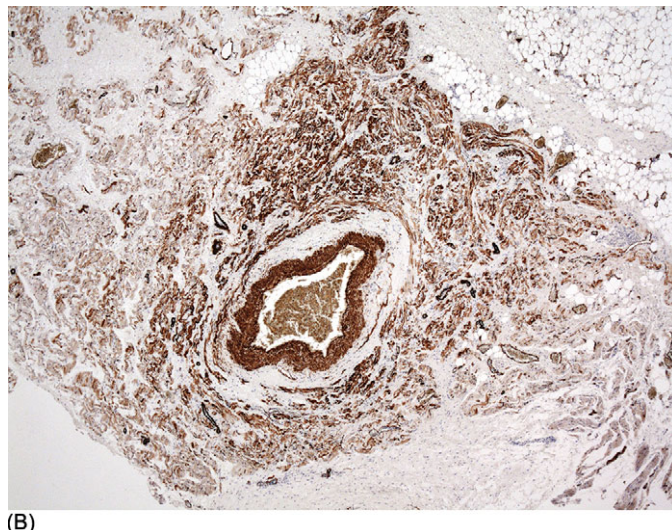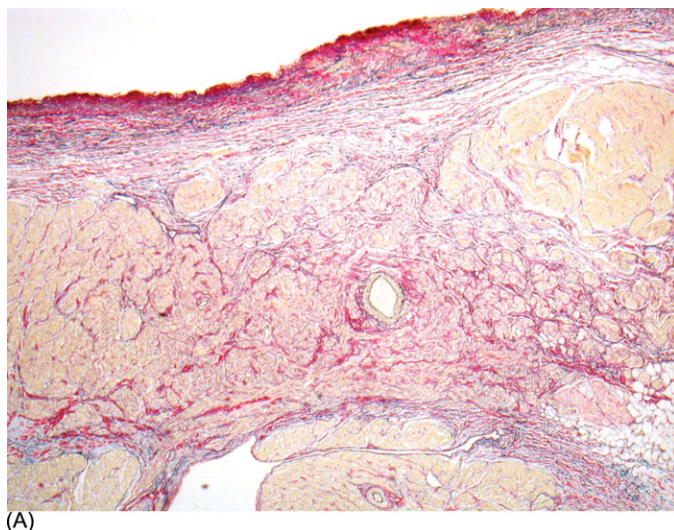
(A)   (B)

Figure 1.72 Histology of normal sinoatrial node. **(A)** The sections show normal sinoatrial node. The epicardial surface is present in the left-hand corner. The node is present as a flat and triangular structure composed of small pale cells centred on the large artery in the centre of the field. It extends almost to the endocardial surface of the atrium in the bottom right-hand corner of the picture. It contains rather more interstitial collagen (stained red) than the surrounding working myocardium. **(B)** Sinoatrial node from a case of sudden childhood death stained with antibody to smooth muscle actin. There is strong staining of the smooth muscle of the central nodal artery. The cells of the node are dispersed around the artery and show cytoplasmic positivity in contrast to the negative cells of the working myocardium.

elastic tissue (Figure 1.75). The origins of the coronary arteries from the aorta show a short segment where the arterial wall structure is a hybrid of muscular and elastic artery (Figure 1.76). At the origins there is often a small amount of intimal thickening, and small areas of intimal thickening with some disruption of the underlying internal elastic lamina are present even in late fetal life. During the first few months of life the epicardial arteries develop irregular intimal thickenings, most pronounced in the left anterior descending artery and at the branch points. These fibrous thickenings contain elastic fibres and cells [39, 40]. They become relatively less conspicuous with the growth in size of the vessels (Figure 1.77). A more detailed discussion of coronary artery histology and its variants is given in Chapter 9.

1.3.7 Cardiac Veins

The cardiac veins have the structure of normal systemic veins (Figure 1.78). The intima is thin and consists of endothelium only. An internal elastic lamina is not readily discernible. The media is not well developed and contains muscle cells, elastic fibres and collagen, but without the orderly arrangement of the arterial wall. It is a thin layer. The adventitia contains abundant collagen and elastic fibres.

1.3.8 Cardiac Lymphatics

There are three lymphatic plexuses in the ventricular myocardium [41], one in the epicardium and one in the endocardium connected by an intramyocardial plexus. The endocardial plexus drains through the myocardium to the epicardial plexus that drains via lymphatics accompanying the major epicardial

arteries (Figure 1.79). The atria appear to have only an epicardial plexus. Lymphatics are present in the valves.

1.3.9 Aorta, Pulmonary Arteries and Arterial Duct

The aorta and pulmonary trunk are both elastic arteries. They show a thick tunica media composed of concentrically arranged sheets of elastic tissue with smooth muscle between them. In histological sections these sheets appear as elastic laminae. The internal elastic lamina is well developed. Internal to it lies the tunica intima that comprises only endothelium lying on the internal elastic lamina. The external elastic lamina is not well formed. The tunica adventitia comprises collagenous fibrous tissue and fine elastic fibres. It contains nerves and small blood vessels and lymphatics. The pulmonary trunk changes its elastic laminae, which before birth are continuous, similar to those in the aorta. In the pulmonary trunk and its main branches the elastic fibres are fragmented, but the smaller elastic pulmonary arteries show continuous laminae (Figure 1.80). Smooth muscle cells lie between the elastic laminae, and the endothelial layer rests on the internal elastic lamina. The arterial duct is a muscular artery that lies between the two elastic arteries: the aorta and pulmonary trunk. The duct has a thick muscular media. In the third trimester its tunica intima develops swellings that contain smooth muscle cells and abundant glycosaminoglycans (mucopolysaccharide) (Figure 1.81). These increase in size and project into the lumen, and the smooth muscle of the media begins to develop pools of glycosaminoglycans also. At birth there is contraction of the arterial duct with apposition of the intimal cushions occluding the lumen. The media becomes fibrotic and eventually calcifies.
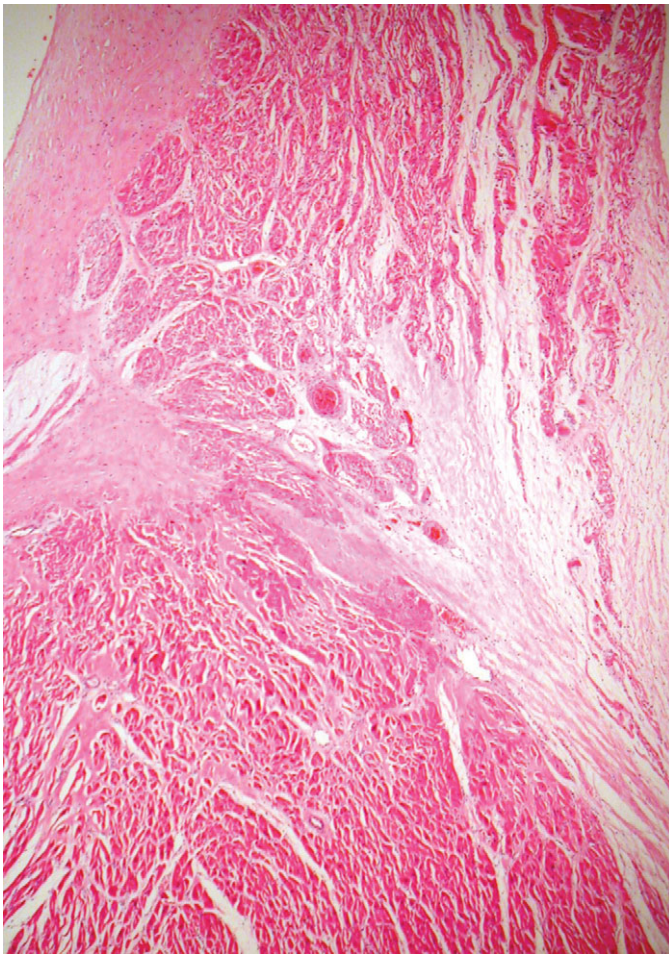
Figure 1.73 Histology of normal AV node. A section through the atrioventricular junction to demonstrate the AV node. The right atrium is to the left and the left atrium to the right. The upper part of the field shows the myocardium of the interatrial septum and the lower part of the field shows the crest of the interventricular septum. A tongue of atrial myocardium descends from the left atrial aspect towards the hinge point to the mitral valve. The node is a triangular area of myocardium identified by the presence of the nodal artery and the relatively small size of the constituent myocytes.

Figure 1.74 Histology of branching bundle of His.

1.3.10 Nerves

Autonomic nerves serve not to cause contraction of the heart muscle, but rather to regulate overall activity.

1.4 Electron Microscopy

The myocytes are cylindrical, about 15 μm in diameter and have an outer plasma membrane with associated basal lamina together forming the sarcolemma. The cytoplasm contains the usual organelles – mitochondria, lysosomes, Golgi and endoplasmic reticulum (termed sarcoplasmic reticulum in the myocyte) – but the most striking feature is the presence of multiple longitudinally arranged contractile elements, the myofibrils (between 300 and 700 per cell) (Figure 1.82). Each of these myofibrils is composed of subsidiary myofilaments (approximately 200–1000 per myofibril), which contain a myosin

filament surrounded by six actin filaments [42]. Within the myofibril the functional unit is the sarcomere, composed of actin and myosin filaments bounded at their ends by Z-bands. Actin filaments from contiguous sarcomeres insert into the Z-band, which serves as an anchoring point for the filaments during contraction (Figure 1.83). Within the myocytes there are invaginations of the plasma membranes and associated basal lamina forming transverse tubules entering the cells. These come into close contact with the sarcoplasmic reticulum. The sarcoplasmic reticulum forms a branching system of tubules within the sarcoplasm that is more or less parallel to the microfilaments and has points of contact with the T system and the sarcolemma. Adjacent myocytes are connected in a step-like fashion by intercalated discs.

The sarcomeres are composed of I-bands formed by thin filaments, A-bands formed by thick filaments and M-bands formed by transversely oriented protein cross bridges that connect adjacent thick filaments and Z-bands composed of finely filamentous electron-dense material. Transversely oriented filaments connect adjacent myofibrils to the nuclear membranes and to the sarcolemma. Nuclei are centrally located and composed of the inner and outer nuclear membranes and nucleoli. The nuclear membrane contains pores.
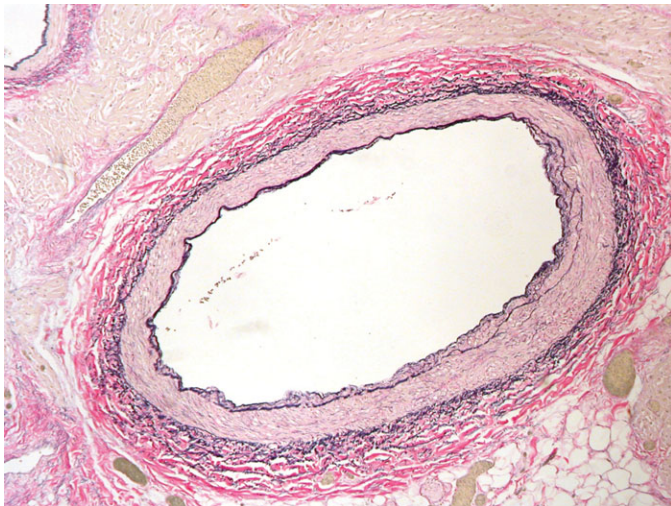
Figure 1.75 Histology of normal epicardial coronary artery. Sudden death case in a five-year-old.

Figure 1.77 Intimal thickening of neonatal coronary arteries.

Figure 1.76 Origin of coronary artery from aorta. It can be appreciated that the first couple of millimetres of the vessel wall has an elastic structure similar to that of the aorta.

The atrial myocardium contains dense core bodies [43] that store the myocytokines atrial natriuretic peptide and brain natriuretic peptide.

Non-myelinated nerves are present in the myocardium, especially adjacent to the node in the right atrium. Lipid droplets and membrane-bound glycogen are present.

Mitochondria are found in three separate locations within the myocyte:

1. Beneath the sarcolemma
2. Between the filaments
3. Perinuclearly

It is thought that they carry out separate functions – energy generation largely for contraction, with ion channel regulation and with transcription respectively [44].

Gap junctions are clusters of channels that span the cell membrane and directly link the cytoplasm of contiguous cells

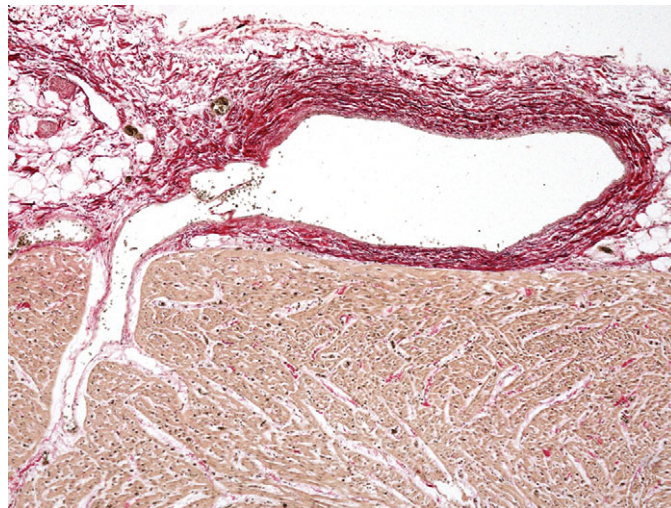**Figure 1.78** Histology of normal cardiac vein. Section of an epicardial vein situated over the anterior aspect of the interventricular septum stained with Elastic vanGieson. Note the paucity of muscle in the wall and the presence of a valve at the junction with the branch emerging from the myocardium.

permitting direct intercellular communication. In the heart, gap junctions also mediate electrical coupling between myocytes. In the heart, gap junctions vary greatly in size, some containing tens of thousands of channels and others fewer than ten. The gap junctions are organised together with two types of adhesion junction – fasciae adherentes junctions and desmosomes – at the intercalated discs (Figure 1.84) [45].

The intercalated disc has a characteristic irregular, step-like structure, specialised for the task of integrating cell-to-cell electro-mechanical function. Fasciae adherentes junctions, which transmit mechanical force from cell to cell, are situated in the vertical "steps" of the disc, linking up the myofibrils of

adjacent cells in series. Desmosomes, often likened to "press studs" between cells, form attachment sites for the desmin cytoskeleton, and are found predominantly in the intervening horizontal portions of the disc. Most of the gap junctions are also found in these horizontal segments, often with larger junctional plaques at the disc periphery.

Each channel in a gap junction comprises a pair of abutting hemichannels, termed connexons, one contributed by each of the apposed cell membranes. The connexon spans the full depth of the membrane and is composed of six connexin molecules. Twenty-one different connexin types have been identified, and the specific connexin type or mix of types within the connexon permits differentiation of the functional properties of the channel.

Cardiac myocytes express three principal connexins: connexin40 (Cx40), Connexin43 (Cx43) and Connexin45 (Cx45). Connexin43 predominates and shows co-expression with Cx40 and/or Cx45. The pattern of expression is specific for the working (contractile) myocardium of atria, ventricles and the specialised conduction tissue [46].

In the working myocytes of the ventricle Cx43-containing gap junctions predominate. In the atrial myocardium gap junctions are organised in less well demarcated intercalated discs and contain both Cx43 and Cx40. In both ventricular and atrial human myocardium, Cx45 is detected in low quantities, with higher levels in the atria than the ventricles.

The myocytes of the conduction system differ from the working myocardium in their connexin expression profiles. Myocytes of the sinoatrial and AV nodes characteristically have small, dispersed gap junctions composed of Cx45. Distal to the bundle of His, the conduction system myocytes co-express Cx40. Cx43 becomes more abundant in the more distal parts of the system, and Cx45 is expressed continuously from the AV node to the ends of the Purkinje fibres.
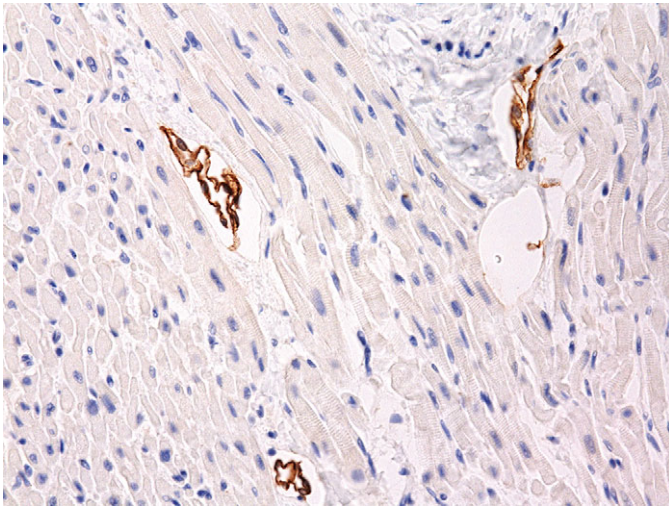
Figure 1.79 Cardiac lymphatic histology. A section through the right ventricular myocardium of a four-year-old – stained with antibody D2–40. This highlights the endothelium of small lymphatic vessels in the superficial myocardium.
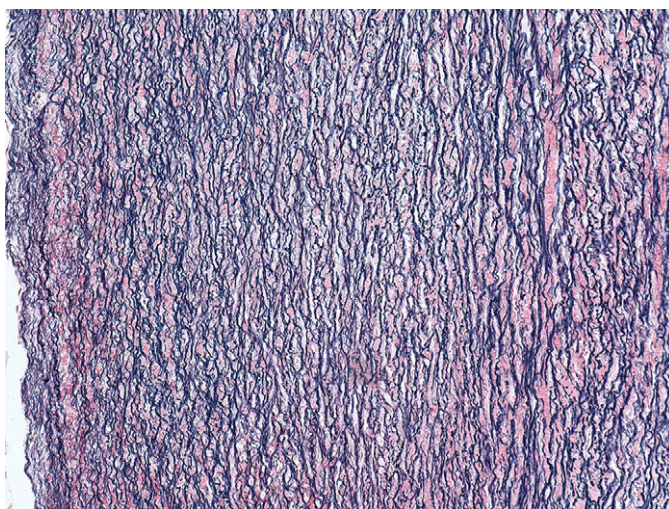
(A)
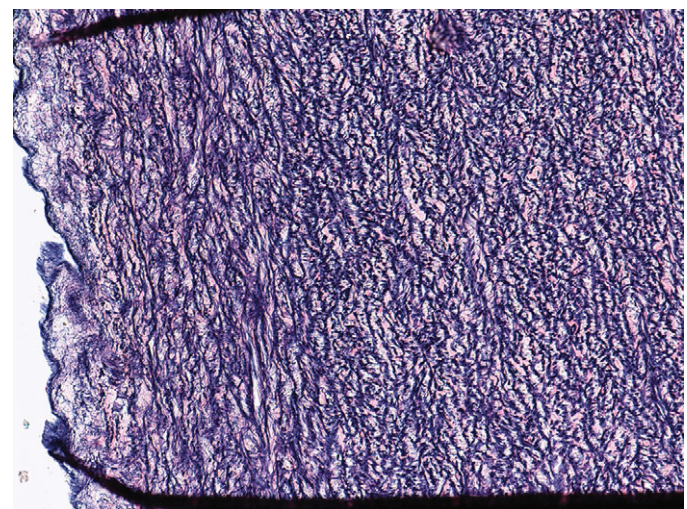
(B)

Figure 1.80 Aorta and pulmonary artery. The pulmonary artery **(A)** and the aorta **(B)** from the same infant heart, stained with Elastic vanGieson (EvG) and photographed at the same magnification. The elastic fibres in the pulmonary artery are finer and shorter than those in the aorta.

27
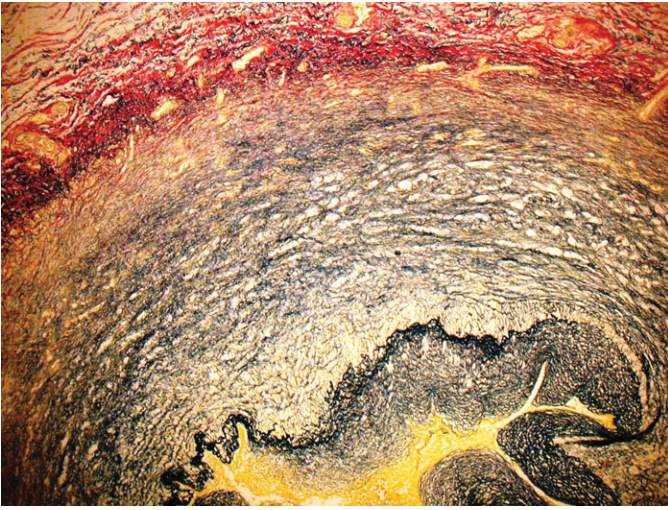
Figure 1.81 Arterial duct at term. A section through part of the wall of the duct at term, stained with Elastic vanGieson. The tunica media contains muscle and is pale. There are intimal cushions that contain abundant elastic tissue. The duct is contracted.
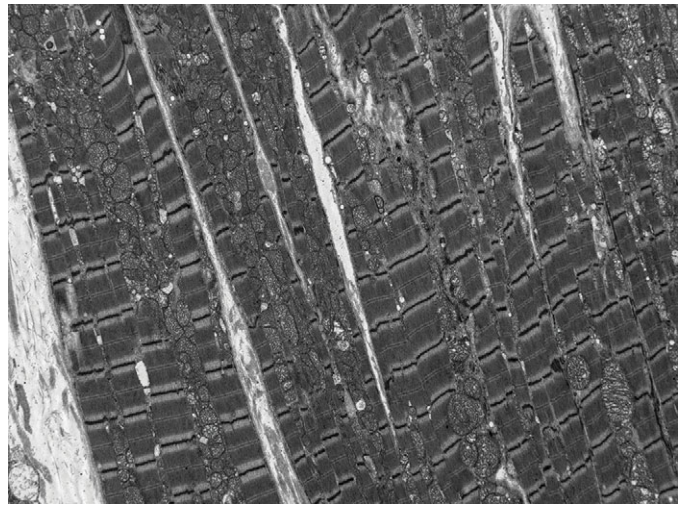
Figure 1.82 Electron microscopy (EM) of myofilaments showing the ultrastructure of longitudinally arranged myocytes. The parallel arrangement of the myofilaments within the myocytes gives the characteristic banded appearance of the myocyte. The mitochondria are arranged running longitudinally between the bundles of myofilaments (Figure courtesy of Mr G. Anderson, Clinical Electron-Microscopist, GOSH).

Figure 1.83 EM of sarcomere. A higher power view shows bundles of myofilaments with intervening mitochondria (Figure courtesy of Mr G. Anderson, Clinical Electron-Microscopist, GOSH).
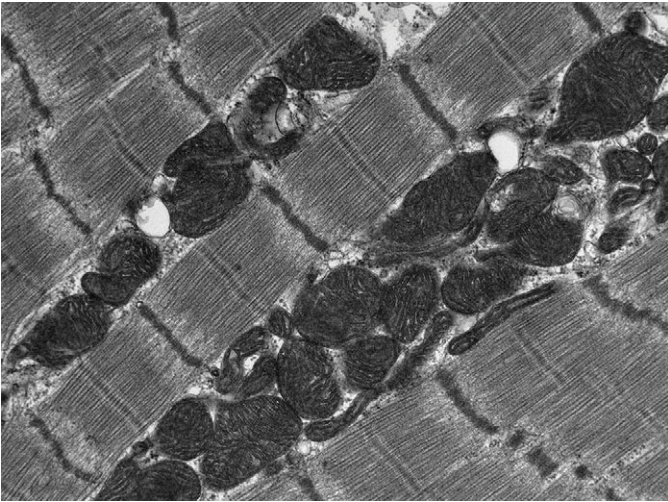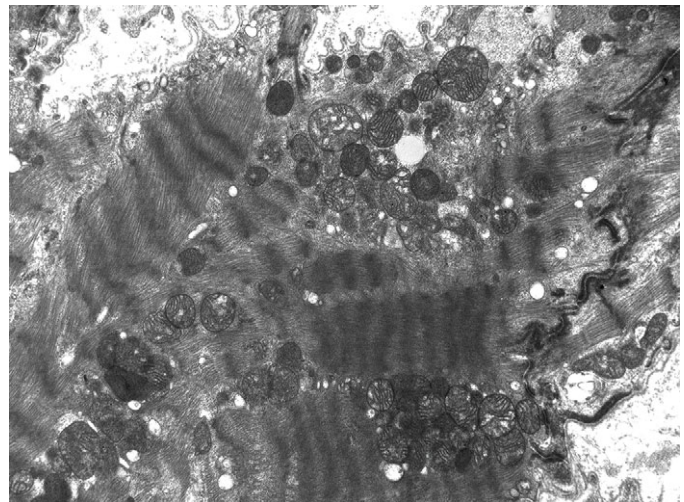

Figure 1.84 EM of intercalated discs. An intercalated disc is seen at the left of the picture consisting of stepped desmosomes visible as dark parallel lines with a pale intervening line. Multiple rounded mitochondria are also seen. A sinuous cell membrane is seen at the top of the field (Figure courtesy of Mr G. Anderson, Clinical Electron-Microscopist, GOSH).

1.5 Weights and Measures

It is possible to record many measurements of the heart. The simplest, and probably the most useful, is the weight. The organ is weighed following evacuation of all blood and blood clot. The heart weight is a reflection of the weight of the myocardium and gives in turn a measure of ventricular myocardial bulk. The heart size, and hence weight, increases in a more or less linear fashion throughout gestation and continues to grow throughout childhood to adulthood.

Standard tables have been available for over half a century giving weights for normal hearts for children and adults [47–50] (Table 1.1). These have been supplemented by tables for the third and second trimester fetus [51, 52]. Tables have also been produced of weights of fetal organs that have been formalin-fixed [53]. Ranges have been produced with centiles, and many centres have sought to establish local ranges to reflect their local populations [54] (Table 1.2). Given the recent rise in body weight among adults, new tables have been prepared to reflect this increase [55]. Body surface area shows a strong relationship to left ventricular mass [56], at least in adults.

Other measurements that may be useful include ventricular wall thickness. This usually entails measuring the thickness of

Table 1.1 Heart measurements related to age and length, males

| Age	Body		Heart	Thickness (cm)		Valve circumferences (cm)			
	Weight (g)	Length (cm)	Weight (g)	Lv	Rv	Tricuspid	Pulmonic	Mitral	Aortic
Gestational age									
5 mo	312	22.7	4.6	0.20	0.20	1.3	0.8	1.2	0.9
6 mo	729	30.6	6.2	0.28	0.20	2.3	1.2	2.0	1.0
7 mo	1145	36.2	9.8	0.35	0.26	2.4	1.4	2.2	1.3
8 mo	1778	40.6	14.0	0.39	0.28	3.1	1.8	2.6	1.6
9 mo	2420	45.0	18.0	0.42	0.30	3.4	2.0	2.9	1.8
Post-natal age									
0–1 wk	3171	49.3	23.0	0.46	0.32	3.8	2.2	3.2	2.0
1 mo		51.4	23.0	0.59	0.26	3.8	2.3	3.3	2.1
2 mo		54.0	27.0	0.60	0.29	4.2	2.5	3.4	2.3
3 mo		57.7	30.0	0.64	0.25	4.4	2.7	3.6	2.6
4 mo		60.4	31.0	0.65	0.23	4.7	2.7	3.8	2.6
5 mo		62.0	35.0	0.68	0.26	4.8	2.9	4.1	2.7
6 mo		64.2	40.0	0.74	0.26	5.0	3.1	4.2	2.8
7 mo		66.7	43.0	0.76	0.28	5.0	3.1	4.2	2.9
8 mo		68.2	44.0	0.76	0.27	5.2	3.2	4.4	3.2
9 mo		69.4	45.0	0.74	0.24	5.4	3.2	4.5	3.0
10 mo		69.7	46.0	0.75	0.26	5.4	3.4	4.5	3.3
11 mo		70.5	48.0	0.73	0.25	5.5	3.3	4.6	3.2
12 mo		73.8	50.0	0.79	0.28	5.5	3.5	4.7	3.3
13–18 mo		78.0	54.0	0.80	0.27	5.8	3.5	4.7	3.4
19–24 mo		84.0	60.0	0.80	0.26	6.2	3.7	5.0	3.5
3 yr		90.0	72.0	0.79	0.27	6.8	4.0	5.5	3.9
4 yr		101.0	88.0	0.86	0.24	7.3	4.5	6.1	4.2
5 yr		109.0	94.0	0.86	0.25	7.5	4.5	6.2	4.4
6 yr		114.0	105.0	0.86	0.24	7.8	4.4	6.1	4.3
7 yr		121.0	110.0	0.92	0.27	7.9	4.7	6.5	4.4
8 yr		127.0	119.0	0.94	0.25	8.3	4.8	6.8	4.7
9 yr		132.0	138.0	1.00	0.28	8.6	4.9	7.2	4.7
10 yr		138.0	150.0	0.98	0.28	8.8	5.2	7.4	4.9
11 yr		144.0	154.0	1.00	0.26	9.6	5.2	7.3	4.9
12 yr		149.0	169.0	1.00	0.25	9.5	5.5	7.8	5.4
13 yr		155.0	212.0	1.03	0.28	10.3	6.2	7.9	5.6
14 yr		159.0	219.0	1.04	0.26	10.6	6.2	8.4	5.8
15 yr		163.0	224.0	1.05	0.27	10.8	6.3	8.3	5.9

Lv, left ventricular; Rv, right ventricular.
Schultz & Giordano. *Arch Pathol* 74: 464–471,1962. [47].

Table 1.2 Heart weight infants. BMC Clin Pathol. 2014; 14: 18 (Ref 53)
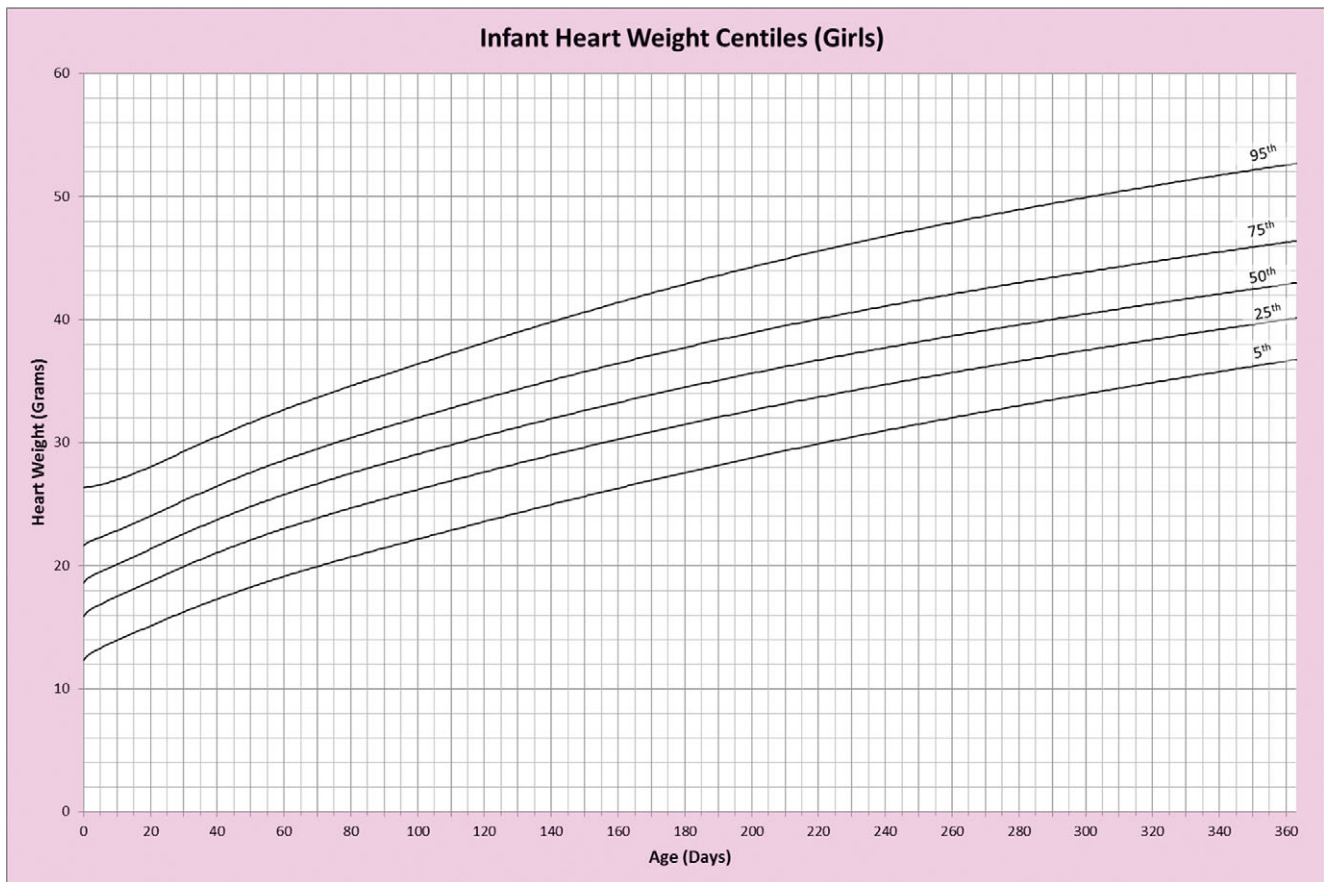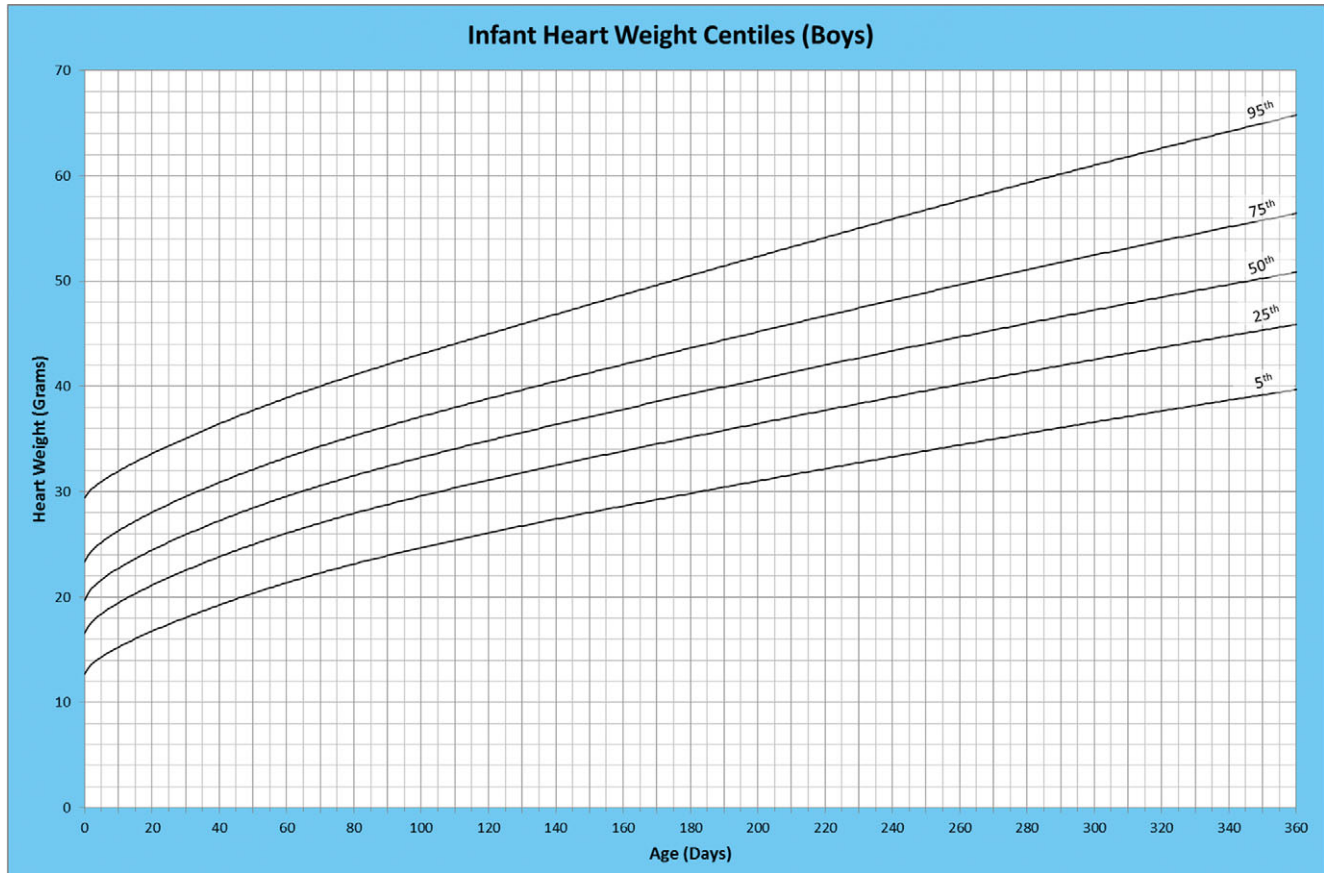
the myocardium of the free wall of the left and right ventricles and of the interventricular septum. This can vary depending on where it is measured, but it has been standardised for echocardiographic and other radiological investigation and it is possible to reproduce this at autopsy. A single measurement is probably not very useful.

The size of valves may be measured with a set of obturators that are introduced into the valve orifice. Alternatively, length and breadth of the orifice may be measured in the unopened valve (or diameter in the case of valves with a circular profile). Additionally, the valve circumference may be measured in the opened valve. Standard tables are available for these measurements in children of varying age [48, 51].

Other measurements that may be useful in individual cases include the maximum diameter of the atria or ventricular chambers where these structures are dilated or contracted. And, of course, the measurements for abnormal features, for example septal defects, should be recorded.

Given the increasing popularity of post-mortem imaging, it is useful to bear in mind that there is evidence that the measurements of heart wall thickness in post-mortem CT are higher than those in ante-mortem CT of the same hearts [57].

References

1. Cabrera JA, Sanchez-Quintana D, Ho SY, Medina A, Anderson RH. The architecture of the atrial musculature between the orifice of the inferior caval vein and the tricuspid valve: the anatomy of the isthmus. *J Cardiovasc Electrophysiol* 1998; **9**: 1186–1195.

2. Jones RN, Niles NR. Spinnaker formation of sinus venosus valve. *Circulation* 1968; **38**: 468–473.

3. Doucette J, Knoblich R. Persistent right valve of the sinus venosus. *Arch Pathol* 1963; **75**: 105–112.

4. Arey JB. Embryology of the heart and great vessels. In *Cardiovascular Pathology in Infants and Children*. Philadelphia: WB Saunders; 1984, p. 25.

5. Restivo A, Smith A, Wilkinson JL, Anderson RH. The medial papillary muscle complex and its related septomarginal trabeculation. A normal anatomical study on human hearts. *J Anat* 1989; **163**: 231–243.

6. Rosenquist GC, Clark EB, Sweeney LJ, McAllister HA. The normal spectrum of mitral and aortic valve discontinuity. *Circulation*.1976; **54**: 298–301.

7. Pomerance A. Atheroma of the mitral valve. *J. Atheroscler Res* 1967; **7**: 151–160.

8. Rosenquist GC, Sweeny LJ, Amsel J et al. Enlargement of the membranous ventricular septum: an internal stigma of Down's syndrome. *J Pediatr* 1974; **85**: 490–493.

9. Jouk PS, Usson Y, Michalowicz G, Grossi L. Three-dimensional cartography of the pattern of the myofibres in the second trimester fetal human heart. *Anat Embryol* 2000; **202**: 103–118.

10. Anderson RH, Ho SY, Smith A et al. Study of the cardiac conduction tissues in the paediatric age group. *Diagn Histopathol* 1981; **4**: 3–15.

11. Blom NA, Gittenberger-de Groot AC, DeRuiter MC et al. Development of the cardiac conduction tissue in human embryos using HNK-1 antigen expression: possible relevance for understanding of abnormal atrial automaticity. *Circulation*. 1999; **99**: 800–806.

12. Anderson RH, Ho SY, Smith A, Becker AE. The internodal atrial myocardium. *Anat Rec* 1981; **201**: 75–82.

13. James TN. Cardiac conduction system: fetal and postnatal development. *Am J Cardiol* 1970; **25**: 213–226.

14. Moulaert AJ, Oppenheimer-Dekker A. Anterolateral muscle bundle of the left ventricle, bulboventricular flange and subaortic stenosis. *Am J Cardiol* 1976; **37**: 78–81.

15. Anderson RH. Surgical anatomy of the coronary circulation. In Wilcox BR, Cook AC, Anderson RH (eds) *Surgical Anatomy of the Heart*, 3rd edn. Cambridge: Cambridge University Press; 2004, pp. 84–85.

16. Schlesinger MJ, Zoll PM, Wessler S. The conus artery: a third coronary artery. *Am Heart J* 1949; **38**: 823–826.

17. Garg A, Ogilvie BC, McLeod AA. Anomalous origin of the left coronary artery from the non-coronary sinus of Valsalva. *Heart* 2000; **84**: 136.

18. Spicer DE, Henderson DJ, Chaudhry B, Mohun TJ, Anderson RH. The anatomy and development of normal and abnormal coronary arteries. *Cardiol Young* 2015; **25**: 1493–1503.

19. von Lüdinghausen M. The venous drainage of the human myocardium. *Adv Anat Embryol Cell Biol* 2003; **168**: I–VIII, 1–104.

20. Loukas M, Bilinsky S, Bilinsky E, el-Sedfy A, Anderson RH. Cardiac veins: a review of the literature. *Clin Anat* 2009; **22**: 129–145.

21. Ho SY, Sanchez-Quintana D, Becker AE. A review of the coronary venous system: a road less travelled. *Heart Rhythm* 2004; **1**: 107–112.

22. Zhou P, Pu WT. Recounting cardiac cellular composition. *Circ Res* 2016; **118**: 368–370.

23. Pinto AR, Ilinykh A, Ivey MJ et al. Revisiting cardiac cellular composition. *Circ Res* 2016; **118**: 400–409.

24. Anderson RH, Smerup M, Sanchez-Quintana D, Loukas M, Lunkenheimer PP. The three-dimensional arrangement of myocytes in the ventricular walls. *Clin Anat* 2009; **22**: 64–76.

25. Stephens WE, Zuccollo JM. Anitschkow myocytes or cardiac histiocytes in human hearts. *Pathology* 1999; **31**: 98–101.

26. Favara BE, Moores H. Anitschkow nuclear structure: a study of pediatric hearts. *Pediatr Pathol* 1987; **7**: 151–164.

27. Goyal VK. Early appearance and rate of lipofuscin pigment accumulation in human myocardium. *Exp Geront* 1981; **16**: 219–222.

28. Douglas YL, Jongbloed MR, Gittenberger-de Groot AC et al. Histology of vascular myocardial wall of left atrial body after pulmonary venous incorporation. *Am J Cardiol* 2006; **97**: 662–670.

29. Smith EB, Butcher J. The incidence, distribution and significance of megakaryocytes in normal and diseased human tissues. *Blood* 1952; **7**: 214–224.

30. Levick SP, Meléndez GC, Plante E et al. Cardiac mast cells: the centrepiece in

adverse myocardial remodelling. *Cardiovasc Res* 2011; **89**(1): 2–19.

31. Acebo E, Val-Bernal JF, Gómez-Román JJ. Prichard's structures of the fossa ovalis are not histogenetically related to cardiac myxoma. *Histopathology* 2001; **39**: 529–535.

32. Val-Bernal JF, Martino M, Mayorga M, Garijo MF. Prichard's structures of the fossa ovalis are age-related phenomena composed of nonreplicating endothelial cells: the cardiac equivalent of cutaneous senile angioma. *APMIS* 2007; **115**: 1234–1240.

33. Hinton RB, Yutzey KE. Heart valve structure in development and disease. *Annu Rev Physiol* 2011; **73**: 29–46.

34. Mirzaie M, Schultz M, Schwartz P, Coulibaly M, Schöndube F. Evidence of woven bone formation in heart valve disease. *Ann Thorac Cardiovasc Surg* 2003; **9**: 163–169.

35. Zimmerman KG, Paplanus SH, Dong S, Nagle RB. Congenital blood cysts of the heart valves. *Hum Pathol* 1983; **14**: 699–703.

36. Gallucci V, Stritoni P, Fasoli G, Thiene G. Giant blood cyst of tricuspid valve. Successful excision in an infant. *Br Heart J* 1976; **38**: 990–992.

37. Cook AC, Fagg NLK, Sharland GK. Large blood cyst causing severe left ventricular obstruction in a fetus. *Cardiol Young* 1996; **6**: 171–173.

38. Anderson KR, Ho SY, Anderson RH. Location and vascular supply of sinus node in human heart. *Br Heart J* 1979; **41**: 28–32.

39. Pesonen E. Extrinsic and intrinsic factors relating to intimal thickening in children. *Acta Paediatr Suppl* 2004; **446**: 43–47.

40. DeSa DJ. Coronary artery ruptures in stillbirths *Pediatr Dev Pathol* 2002; **5**: 605.

41. Loukas M, Abel M, Tubbs RS et al. The cardiac lymphatic system. *Clin Anat* 2011; **24**: 684–691.

42. Sommer JR, Waugh RA. Ultrastructure of heart muscle. *Environ Health Perspect* 1978; **26**: 159–167.

43. Chiba A, Watanabe-Takano H, Miyazaki T, Mochizuki N. Cardiomyokines from the heart. *Cell Mol Life Sci* 2018; **75**: 1349–1362.

44. Hoppel CL, Tandler B, Fujioka H, Riva A. Dynamic organization of mitochondria in human heart and in myocardial disease. *Int J Biochem Cell Biol* 2009; **41**: 1949–1956.

45. Severs NJ, Bruce AF, Dupont E, Rothery S. Remodelling of gap junctions and connexin expression in diseased myocardium. *Cardiovasc Res* 2008; **80**: 9–19.

46. Desplantez T. Cardiac Cx43, Cx40 and Cx45 co-assembling: involvement of connexins epitopes in formation of hemichannels and Gap junction channels. *BMC Cell Biol* 2017; **18**: 3.

47. Schulz DM, Giordano DA, Schulz DH. Weights of organs of fetuses and infants. *Arch Pathol* 1962; **74**: 244–250.

48. Rowlatt UF, Rimoldi HJA, Lev M. The quantitative anatomy of the normal child's heart. *Pediatr Clin N Am* 1963; **10**: 499–588.

49. Eckner FAO, Brown BW, Davidson DL, Glagov S. Dimensions of normal human hearts. *Arch Pathol Lab Med* 1969; **88**: 497–507.

50. Sholtz DG, Kitzman DW, Hagen PT, Ilstrup DM, Edwards WD. Age related changes in normal human hearts during the first 10 decades of life. Part I (growth): a quantitative anatomic study of 200 specimens from subjects from birth to 19 years old. *Mayo Clin Proc* 1988; **63**: 126.

51. Alvarez L, Aránega A, Saucedo R, Contreras JA. The quantitative anatomy of the normal human heart in fetal and perinatal life. *Int J Cardiol* 1987; **17**: 57–72.

52. Hanson K, Sung CJ, Huang C et al. Reference values for second trimester fetal and neonatal organ weights and measurements. *Ped Devel Pathol* 2003; **6**:160 – 167.

53. Guihard-Costa AM, Ménez F, Delezoide AL. Organ weights in human fetuses after formalin fixation: standards by gestational age and body weight. *Pediatr Dev Pathol* 2002; **5**: 559–578.

54. Pryce JW, Bamber AR, Ashworth MT et al. Reference ranges for organ weights of infants at autopsy: results of >1,000 consecutive cases from a single centre. *BMC Clin Pathol* 2014; **14**: 18.

55. Gaitskell K, Perera R, Soilleux EJ. Derivation of new reference tables for human heart weights in light of increasing body mass index. *J Clin Pathol* 2011; **64**: 358–362.

56. Hees PS, Fleg JL, Lakatta EG, Shapiro EP. Left ventricular remodeling with age in normal men versus women: novel insights using three-dimensional magnetic resonance imaging. *Am J Cardiol* 2002; **90**: 1231–1236.

57. Okuma H, Gonoi W, Ishida M et al. Heart wall is thicker on postmortem computed tomography than on antemortem [corrected] computed tomography: the first longitudinal study. *PLoS ONE* 2013; **8**: e76026.